Constr. Approx. (2000) 16: 221–259
DOI: 10.1007/s003659910010

CONSTRUCTIVE APPROXIMATION

Biorthogonal Multiwavelets on the Interval: Cubic Hermite Splines

W. Dahmen, B. Han, R.-Q. Jia, and A. Kunoth

Abstract. Starting with Hermite cubic splines as the primal multigenerator, first a dual multigenerator on $\mathbb{R}$ is constructed that consists of continuous functions, has small support, and is exact of order 2. We then derive multiresolution sequences on the interval while retaining the polynomial exactness on the primal and dual sides. This guarantees moment conditions of the corresponding wavelets. The concept of stable completions [CDP] is then used to construct the corresponding primal and dual multiwavelets on the interval as follows. An appropriate variation of what is known as a hierarchical basis in finite element methods is shown to be an initial completion. This is then, in a second step, projected into the desired complements spanned by compactly supported biorthogonal multiwavelets. The masks of all multigenerators and multiwavelets are finite so that decomposition and reconstruction algorithms are simple and efficient. Furthermore, in addition to the Jackson estimates which follow from the exactness, one can also show Bernstein inequalities for the primal and dual multiresolutions. Consequently, sequence norms for the coefficients based on such multiwavelet expansions characterize Sobolev norms $\|\cdot\|_{H^s([0,1])}$ for $s \in (-0.824926, 2.5)$. In particular, the multiwavelets form Riesz bases for $L_2([0,1])$.

1. Introduction

An important ingredient for extending wavelet concepts to problems defined on bounded domains is the construction of wavelets on the interval, see, e.g., [D4]. So far, such constructions have been confined (except for very special cases [SS1]) to wavelets which result from multiresolution analyses built from a single *generator*. Recently, multiresolution spaces have been intensely investigated which are spanned by a so-called *multigenerator*, that is, integer translates of dilates of a finite number of functions satisfying vector refinement relations, see, e.g., [GHM], [GL], [PS2]. The use of a multigenerator appears to be attractive since their component functions have relatively small support and in many cases have more favorable symmetry properties. A particularly interesting case concerns multigenerators consisting of piecewise $\mathcal{C}^1$ cubics. In fact, one can then resort to the powerful tools developed in the spline con-

Date received: February 2, 1998. Date revised: February 19, 1999. Date accepted: March 5, 1999. Communicated by Albert Cohen.
AMS classification: 41A25, 42A38, 39B62.
Key words and phrases: Hermite cubic splines, Biorthogonal multigenerator, Multiwavelets, Interval, Stable completion.

text, and local schemes for interpolating function and derivative data are available. Moreover, the interpolatory nature of the generators suggests convenient ways of adjoining different local tensor product bases by isoparametric mappings, thereby obtaining multiresolution analyses on more complex geometries. Therefore, we concentrate in this paper on the construction of biorthogonal multiwavelets on the interval $[0, 1]$, generated by special $\mathcal{C}^1$ piecewise Hermite cubics, with the following properties:

(I) The primal multiresolution consists of spline spaces of degree 3.
(II) The primal multigenerator and its derivative satisfy interpolation conditions.
(III) By (I), the biorthogonal spline multiwavelets have two vanishing moments.
(IV) The dual multigenerator is continuous and reproduces linear polynomials.
(V) The primal and dual multigenerators and multiwavelets have compact support so that decomposition and reconstruction algorithms are simple and fast.
(VI) The multiwavelets form Riesz bases for $L_2([0, 1])$. Discrete norms based on their expansions characterize Sobolev spaces $H^s([0, 1])$ for $s \in (-0.824926, 2.5)$.

The first important step consists of identifying corresponding biorthogonal multiresolution spaces defined on all of $\mathbb{R}$. Once an appropriate dual multigenerator has been constructed, we proceed to adapt these multigenerators to the interval, resorting to the strategy of preserving polynomial exactness on the primal *as well as* on the dual side [DKU1]. Knowing only the biorthogonal generator bases, we will then construct multiwavelet bases on the interval, all having small support, by projecting certain initial complement functions into the desired ones. The resulting wavelet bases consist again of shift-invariant functions supported in the interior of the interval and a finite number of boundary adapted multiwavelets. We emphasize that the construction automatically generates shift-invariant multiwavelets on $\mathbb{R}$ with small support given by the interior basis functions.

This paper is structured as follows. In Section 2, we collect some facts about the $\mathcal{C}^1$ piecewise Hermite cubics that we use as a multigenerator. We then construct in Section 3 a multigenerator dual to this with small support that consists of continuous functions and reproduces polynomials up to order 2. The first part of the construction of the primal and dual multiresolutions on the interval in Section 4 follows essentially known ideas [AHJP], [CDV], [DKU1]. Near the boundary, one constructs adapted functions as fixed linear combinations of all translates overlapping the boundary in such a way that the polynomial exactness is maintained. This has to be done in order to match the cardinality of the functions on the primal and dual sides. We then perform local changes of bases on the primal and dual sides to recover the interpolation conditions and the biorthogonality near the boundary. The transformation matrices are computed explicitly. In order to derive the multiwavelets and their duals, the concept of stable completions [CDP] is used in Section 5. A variation of hierarchical bases provides an initial stable completion. It can be seen that all mask matrices are banded with band width independent of the refinement level, so that reconstruction and decomposition algorithms are efficient and fast.

To our knowledge, this is the first construction of multiwavelets on the interval for the case where simple restriction is not sufficient.

2. The Primal Multigenerator on $\mathbb{R}$

Consider the functions denoted as *piecewise Hermite cubics* which are defined by

$$\varphi_1(t) := \begin{cases}(t+1)^2(-2t+1), & t \in [-1,0],\\ (1-t)^2(2t+1), & t \in [0,1],\end{cases} \tag{2.1}$$

$$\varphi_2(t) := \begin{cases}(t+1)^2 t, & t \in [-1,0],\\ (1-t)^2 t, & t \in [0,1],\end{cases}$$

and satisfy

$$\varphi_1(k) = \delta_{0,k}, \quad \varphi_2'(k) = \delta_{0,k}, \quad \varphi_1'(k) = 0, \quad \varphi_2(k) = 0 \qquad \text{for all } k \in \mathbb{Z}, \tag{2.2}$$

see Figure 1, where $\delta_{i,k} = 1$ for $i = k$ and $\delta_{i,k} = 0$ otherwise, $i, k, \in \mathbb{Z}$.

Integer translates of φ_1, φ_2 generate the space of $\mathcal{C}^1$-continuous piecewise cubic functions on $\mathbb{R}$ which interpolate function values and first derivatives at $k \in \mathbb{Z}$.

In general, we say that the vector field $\boldsymbol{\varphi}$: $\mathbb{R} \to \mathbb{R}^2$, $\boldsymbol{\varphi} = (\varphi_1, \varphi_2)^T$, constitutes a *multigenerator* if:

(a) the integer translates $\{\boldsymbol{\varphi}(\cdot - k),\ k \in \mathbb{Z}\}$ form an L_2-stable basis for the space

$$S_0 := \mathrm{clos}_{L_2}(\mathrm{span}\{\varphi_i(\cdot - k),\ k \in \mathbb{Z},\ i = 1, 2\}),$$

i.e., for $\mathbf{c} = \{c_{i,k}\}_{i=1,2,\, k\in\mathbb{Z}} \in \ell_2(\{1,2\} \times \mathbb{Z})$, $\mathbf{c}_k := (c_{1,k}, c_{2,k})^T$,

$$\left\| \sum_{k\in\mathbb{Z}} \mathbf{c}_k^T \boldsymbol{\varphi}(\cdot - k) \right\|_{L_2(\mathbb{R})} := \left\| \sum_{k\in\mathbb{Z}} \sum_{i=1}^{2} c_{i,k}\varphi_i(\cdot - k) \right\|_{L_2(\mathbb{R})} \sim \|\mathbf{c}\|_{\ell_2(\mathbb{Z})}. \tag{2.3}$$

(b) $\boldsymbol{\varphi}$ satisfies the *refinement equation*

$$\boldsymbol{\varphi}(x) = \sum_{k\in\mathbb{Z}} \mathbf{A}_k \boldsymbol{\varphi}(2x - k), \qquad x \in \mathbb{R} \quad \text{a.e.}, \tag{2.4}$$

with *mask* $\mathbf{A} := \{\mathbf{A}_k\}_{k\in\mathbb{Z}}$, $\mathbf{A}_k \in \mathbb{R}^{2\times 2}$.

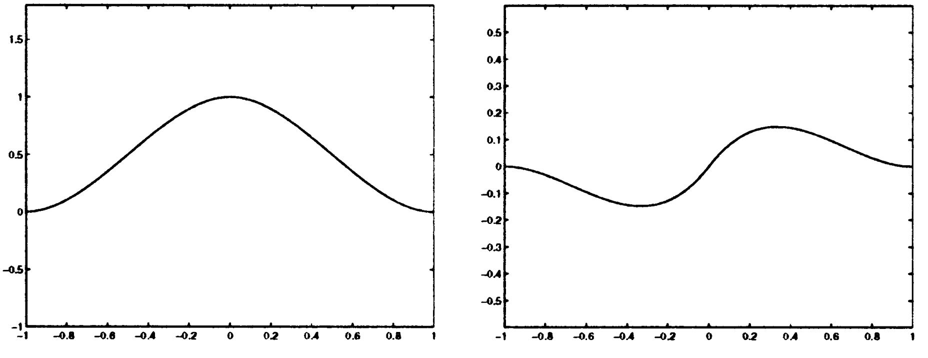

Fig. 1. Multigenerator $\boldsymbol{\varphi} = (\varphi_1, \varphi_2)^T$ on $\mathbb{R}$.

We always mean by $a \sim b$ that $a \lesssim b$ and $b \lesssim a$ hold, where $a \lesssim b$ says that a can be bounded by a constant multiple of b uniformly in any parameters on which a, b may depend, and $a \gtrsim b$ means $b \lesssim a$.

In view of the interpolation conditions, the integer translates of the φ_i, $i = 1, 2$, are linearly independent and hence stable [JM]. The nestedness of the corresponding spline spaces therefore ensures that the piecewise Hermite cubics defined in (2.1) constitute a multigenerator, see also [HSS], [DM]. Multiresolution generated by multigenerators has already been discussed in [JS]. In particular, if $\boldsymbol{\varphi} = (\varphi_1, \dots, \varphi_r)^T$ is a refinable vector of compactly supported functions in $L_2(\mathbb{R})$, and if S_0 is the shift-invariant space generated by $\varphi_1, \dots, \varphi_r$, then it was proved in [JS] that the spaces S_j, $j \in \mathbb{Z}$, spanned by the integer translates of $\varphi_i(2^j \cdot -k)$, $i = 1, \dots, r$, form a multiresolution of $L_2(\mathbb{R})$.

In the following, we will always denote by $\boldsymbol{\varphi}$ the special multigenerator consisting of the functions (2.1). We now proceed by collecting a few properties of the multigenerator that will be needed later.

$\boldsymbol{\varphi}$ satisfies the refinement equation (2.4) with mask matrices

$$\mathbf{A}_{-1} = \begin{bmatrix} \frac{1}{2} & \frac{3}{4} \\ -\frac{1}{8} & -\frac{1}{8} \end{bmatrix}, \qquad \mathbf{A}_0 = \begin{bmatrix} 1 & 0 \\ 0 & \frac{1}{2} \end{bmatrix}, \qquad \mathbf{A}_1 = \begin{bmatrix} \frac{1}{2} & -\frac{3}{4} \\ \frac{1}{8} & -\frac{1}{8} \end{bmatrix}, \tag{2.5}$$

see, e.g., [HSS], such that $\operatorname{supp} \mathbf{A} := \{k \in \mathbb{Z}\colon \mathbf{A}_k \neq \mathbf{0}\} = \{-1, 0, 1\}$. Here boldface numbers will always denote vectors or matrices with all entries equal to this number. Thus, $\boldsymbol{\varphi}$ has compact support $\operatorname{supp} \boldsymbol{\varphi} := \bigcup_{i=1}^{2} \operatorname{supp} \varphi_i = [-1, 1]$. The *symbol* $\mathbf{A}(z)$ relative to the mask $\mathbf{A}$ is defined as $\mathbf{A}(z) = \sum_{k=-1}^{1} \mathbf{A}_k z^k$, $z \in \mathbb{C}\backslash\{0\}$. Note that the normalization of the mask $\mathbf{A}$ differs from the one used in [PS1], [SS2]. Defining the *subsymbols* of $\mathbf{A}(z)$ by $\mathbf{A}_e(z) = \sum_{k=-1}^{1} \mathbf{A}_{2k+e} z^k$, $e = 0, 1$, we know from [DM] that $\mathbf{y} = (1, 0)^T$ is the common left eigenvector of $\mathbf{A}_e(1)$, $e = 0, 1$, for the simple eigenvalue 1.

When saying that $\boldsymbol{\varphi}$ is *symmetric*, we mean that its *member functions* φ_i are either symmetric or antisymmetric. Here we have that $\varphi_1(x) = \varphi_1(-x)$ and $\varphi_2(x) = -\varphi_2(-x)$, which we will abbreviate as

$$\boldsymbol{\varphi}(x) = \mathbf{J}\boldsymbol{\varphi}(-x), \tag{2.6}$$

using

$$\mathbf{J} := \begin{bmatrix} 1 & 0 \\ 0 & -1 \end{bmatrix}. \tag{2.7}$$

The symmetry of the generators carries over to the mask matrices in the sense

$$\mathbf{A}_k = \mathbf{J}\mathbf{A}_{-k}\mathbf{J}, \qquad k = -1, \dots, 1. \tag{2.8}$$

The multigenerator $\boldsymbol{\varphi}$ is normalized such that

$$\int_{\mathbb{R}} \boldsymbol{\varphi}(x)\, dx := \begin{bmatrix} \int_{\mathbb{R}} \varphi_1(x)\, dx \\ \int_{\mathbb{R}} \varphi_2(x)\, dx \end{bmatrix} = \begin{bmatrix} 1 \\ 0 \end{bmatrix}. \tag{2.9}$$

3. A Dual Multigenerator on $\mathbb{R}$

Now we will determine a second compactly supported vector field $\tilde{\varphi}$: $\mathbb{R} \to \mathbb{R}^2$ of continuous functions that is refinable with mask $\tilde{\mathbf{A}}$ and that is *dual* to φ, i.e.,

$$(\varphi, \tilde{\varphi}(\cdot - k))_{\mathbb{R}} = \delta_{0,k}\mathbf{I}, \qquad k \in \mathbb{Z}. \tag{3.1}$$

Here for any domain $\Omega \subset \mathbb{R}$ $(f, g)_\Omega := \int_\Omega f(x)g(x)\, dx$, and for any two vectors $\mathbf{x}, \mathbf{y} \in \mathbb{R}^2$ the term $(\mathbf{x}, \mathbf{y})_{\mathbb{R}}$ denotes the 2×2 matrix with entries $(x_i, y_k)_{\mathbb{R}}$.

It was observed in [DM] that linear independence of the integer translates of the φ_i, $i = 1, 2$, is a necessary condition for the existence of a dual vector of compactly supported functions $\tilde{\varphi}$. In the recent paper [J], it was shown that linear independence is also sufficient for the existence of a compactly supported refinable dual vector of functions in $L_2(\mathbb{R})$.

The strategy for the construction of $\tilde{\varphi}$ is to first solve the discrete analog of (3.1). If $\tilde{\varphi}$ is the unique solution of

$$\tilde{\varphi}(x) = \sum_{k\in\mathbb{Z}} \tilde{\mathbf{A}}_k \tilde{\varphi}(2x - k), \qquad x \in \mathbb{R} \quad \text{a.e.}, \tag{3.2}$$

such that $\int_{\mathbb{R}} \tilde{\varphi}(x)\, dx = [1, 0]^T$, then (3.1) implies

$$\sum_{k\in\mathbb{Z}} \mathbf{A}_k \tilde{\mathbf{A}}^T_{k+2m} = 2\delta_{0,m}\, \mathbf{I} \qquad \text{for all} \quad m \in \mathbb{Z}, \tag{3.3}$$

see [DM]. The construction in [SS2] starts from this equation in symbol form. However, the multigenerator constructed there is not biorthogonal to the Hermite cubic splines φ defined in (2.1). Actually, the Hermite cubic splines are biorthogonal to the third (distributional) derivative of the multigenerator constructed in [SS2]. However, the components of this third derivative are not functions in $L_2(\mathbb{R})$.

Here we choose $\tilde{\mathbf{A}}$ to be the sequence supported on $\{-2, \dots, 2\}$ given by

$$\begin{gathered}\tilde{\mathbf{A}}_{-2} = \begin{bmatrix} -\frac{7}{64} & -\frac{5}{64} \\ \frac{87}{128} & \frac{31}{64} \end{bmatrix}, \qquad \tilde{\mathbf{A}}_{-1} = \begin{bmatrix} \frac{1}{2} & \frac{3}{16} \\ -\frac{99}{32} & -\frac{37}{32} \end{bmatrix}, \qquad \tilde{\mathbf{A}}_{0} = \begin{bmatrix} \frac{39}{32} & 0 \\ 0 & \frac{15}{8} \end{bmatrix}, \\ \tilde{\mathbf{A}}_{1} = \begin{bmatrix} \frac{1}{2} & -\frac{3}{16} \\ \frac{99}{32} & -\frac{37}{32} \end{bmatrix}, \qquad \tilde{\mathbf{A}}_{2} = \begin{bmatrix} -\frac{7}{64} & \frac{5}{64} \\ -\frac{87}{128} & \frac{31}{64} \end{bmatrix}.\end{gathered} \tag{3.4}$$

It is easily verified that this set of matrices satisfies (3.3) with $\mathbf{A}$ from (2.5). Furthermore, the mask coefficients $\tilde{\mathbf{A}}_k$ fulfill

$$\mathbf{M} := \frac{1}{2} \sum_{k\in\mathbb{Z}} \tilde{\mathbf{A}}_k = \begin{bmatrix} 1 & 0 \\ 0 & \sigma \end{bmatrix} \tag{3.5}$$

for some $|\sigma| < 1$. The matrices $\tilde{\mathbf{A}}_{-2} + \tilde{\mathbf{A}}_0 + \tilde{\mathbf{A}}_2$ and $\tilde{\mathbf{A}}_{-1} + \tilde{\mathbf{A}}_1$ have the common left eigenvector $\mathbf{y} = (1, 0)^T$ for the simple eigenvalue 1.

In order to obtain from the discrete biorthogonality relation (3.3) a dual multigenerator $\tilde{\varphi}$, we will employ the concept of subdivision.

3.1. *Existence, Uniqueness, and Regularity of* $\tilde{\varphi}$

Denote by $Q_{\tilde{\mathbf{A}}}$ the bounded linear operator on $L_2(\mathbb{R})^2$ $(:= L_2(\mathbb{R}) \times L_2(\mathbb{R}))$ given by

$$Q_{\tilde{\mathbf{A}}}\mathbf{f} := \sum_{m\in\mathbb{Z}} \tilde{\mathbf{A}}_m \mathbf{f}(2\cdot -m), \qquad \mathbf{f} = (f_1, f_2)^T \in L_2(\mathbb{R})^2. \tag{3.1.1}$$

Let $\mathbf{y}^T = (y_1, y_2) \neq \mathbf{0}$ be a left eigenvector of $\mathbf{M}$ defined in (3.5) corresponding to the eigenvalue 1, i.e., $\mathbf{y}^T\mathbf{M} = \mathbf{y}^T$. We say that the (vector) subdivision scheme associated with $\tilde{\mathbf{A}}$, denoted by $S_{\tilde{\mathbf{A}}}$, *converges in* L_2 if there exists a vector $\mathbf{f} \in L_2(\mathbb{R})^2$ such that for any $\mathbf{f}_0 \in L_2(\mathbb{R})^2$ satisfying

$$\mathbf{y}^T \sum_{m\in\mathbb{Z}} \mathbf{f}_0(\cdot - m) = 1,$$

the sequence $Q^k_{\tilde{\mathbf{A}}}\mathbf{f}_0$ $(:= Q_{\tilde{\mathbf{A}}}(Q^{k-1}_{\tilde{\mathbf{A}}}\mathbf{f}_0))$ converges to $\mathbf{f}$ in the L_2-norm as $k \to \infty$. Then $Q_{\tilde{\mathbf{A}}}\mathbf{f} = \mathbf{f}$ and $\mathbf{f}$ is a solution of the refinement equation (3.2).

Proposition 3.1. *The subdivision scheme* $S_{\tilde{\mathbf{A}}}$ *converges in* L_2.

Proof. Let $\ell_0(\mathbb{Z})$ denote the linear space of all finitely supported sequences on $\mathbb{Z}$ and $\ell_0(\mathbb{Z})^{2\times 2}$ the linear space of all finitely supported sequences of 2×2 matrices. Let $F_{\tilde{\mathbf{A}}}$ be the *transition operator* on $\ell_0(\mathbb{Z})^{2\times 2}$ defined by

$$(F_{\tilde{\mathbf{A}}}\mathbf{C})_k := \frac{1}{2} \sum_{m,s\in\mathbb{Z}} \tilde{\mathbf{A}}_{2k-m}\, \mathbf{C}_{m+s}\, \tilde{\mathbf{A}}_s^T, \qquad k \in \mathbb{Z}, \quad \mathbf{C} \in \ell_0(\mathbb{Z})^{2\times 2}. \tag{3.1.2}$$

Let δ denote the sequence satisfying $\delta_0 = 1$ and let $\delta_m = 0$ for $m \neq 0$. Employing the second-order difference operator Δ, define the sequence $(\Delta\delta)_k := -\delta_{k-1} + 2\delta_k - \delta_{k+1}$. Furthermore, for $i = 1, 2$, let $\mathbf{e}^i$ be the ith unit vector. Recall from [JRZ2, Theorem 7.1], that the subdivision scheme $S_{\tilde{\mathbf{A}}}$ converges in L_2 if and only if $\rho(F_{\tilde{\mathbf{A}}}|_W) < 1$, where W is the minimal invariant subspace of $F_{\tilde{\mathbf{A}}}$ generated by the matrix-valued sequences $\mathbf{e}^1(\mathbf{e}^1)^T\Delta\delta$ and $\mathbf{e}^2(\mathbf{e}^2)^T\delta$, and $\rho(F_{\tilde{\mathbf{A}}}|_W)$ is the spectral radius of $F_{\tilde{\mathbf{A}}}$ restricted to W. By numerical computation, we obtain $\rho(F_{\tilde{\mathbf{A}}}|_W) < 1$ and, thus, the assertion. ■

Proposition 3.2. *The refinement equation* (3.2) *for the mask* $\tilde{\mathbf{A}}$ *defined in* (3.4) *has a unique solution* $\tilde{\boldsymbol{\varphi}}$ *satisfying* (3.1). *Furthermore,* $\tilde{\boldsymbol{\varphi}}$ *is in the Sobolev space* $H^s(\mathbb{R})^2$ *for any*

$$s < \tilde{\gamma} := 0.824926. \tag{3.1.3}$$

In particular, $\tilde{\boldsymbol{\varphi}}$ *consists of continuous functions.*

Proof. It was pointed out in [DM, Theorem 4.1], (see also [JRZ2, Theorem 8.1]), that if the refinement masks $\mathbf{A}$ and $\tilde{\mathbf{A}}$ satisfy (3.3) and if the subdivision schemes associated with $\mathbf{A}$ and $\tilde{\mathbf{A}}$ are convergent in L_2, then there exists a refinable vector $\tilde{\boldsymbol{\varphi}}$ which is the unique solution of the refinement equation (3.2) with mask $\tilde{\mathbf{A}}$, and the duality relation (3.1) holds.

Let, for a function vector $\mathbf{f} \in L_p(\mathbb{R})^2 := L_p(\mathbb{R}) \times L_p(\mathbb{R})$, $\nu_p(\mathbf{f}) := \sup\{\nu\colon \mathbf{f} \in W_p^\nu(\mathbb{R})^2\}$ denote the optimal (Sobolev) regularity of $\mathbf{f}$. By the embedding theorem, one has $\nu_\infty(\mathbf{f}) \geq \nu_2(\mathbf{f}) - \frac{1}{2}$. In order to determine $\nu_2(\tilde{\boldsymbol{\varphi}})$, we review some results from [JRZ2] and [JRZ3]. With the notation from the previous proof we obtain, by [JRZ3, Theorem 3.4],

$$\nu_2(\tilde{\boldsymbol{\varphi}}) = -\tfrac{1}{2}\log_2(\rho(F_{\tilde{\mathbf{A}}}|_V)), \tag{3.1.4}$$

where V is the minimal invariant subspace of $F_{\tilde{\mathbf{A}}}$ generated by $\mathbf{e}^1(\mathbf{e}^1)^T\Delta\delta$ and $\mathbf{e}^2(\mathbf{e}^2)^T\Delta\delta$. Let $\mathbf{v}^0 := \mathbf{e}^1(\mathbf{e}^1)^T\Delta\delta$ and $\mathbf{v}^i := F_{\tilde{\mathbf{A}}}^i\mathbf{v}^0$ for $i \in \mathbb{N}$. We find that V is the linear span of $\mathbf{v}^0, \ldots, \mathbf{v}^8$ and has dimension 9. By using MAPLE we obtain $\mathbf{v}^9 = \sum_{i=0}^{8} h_i\mathbf{v}^i$, where

$$h_0 = \frac{121393}{30223145490365729367654 4}, \quad h_1 = \frac{12707291903433}{2361183241434822606848},$$

$$h_2 = -\frac{12781989485512689}{1888946593147858085478 4}, \quad h_3 = \frac{1509351271768101}{1475739525896764129 28},$$

$$h_4 = -\frac{129495711992289}{288230376151711744}, \qquad h_5 = \frac{403668071727}{281474976710656},$$

$$h_6 = \frac{2701056849}{137438953472}, \qquad h_7 = -\frac{13306731}{67108864},$$

$$h_8 = \frac{381}{512}.$$

Therefore, the characteristic polynomial $P(z)$ of the linear operator $F_{\tilde{\mathbf{A}}}$ under the basis $\mathbf{v}^0, \ldots, \mathbf{v}^8$ is given by $P(z) = z^9 - \sum_{i=0}^{8} h_i z^i$. By numerical computation, we find that the largest absolute value of the roots of $P(z)$ is approximately 0.31867282. Hence $\rho(F_{\tilde{\mathbf{A}}}|_V) \approx 0.31867282$, and thus by (3.1.4)

$$\nu_2(\tilde{\boldsymbol{\varphi}}) = -\tfrac{1}{2}\ \log_2(\rho(F_{\tilde{\mathbf{A}}}|_V)) \approx 0.824926 = \tilde{\gamma}. \tag{3.1.5}$$

It follows that $\nu_\infty(\tilde{\boldsymbol{\varphi}}) \geq \nu_2(\tilde{\boldsymbol{\varphi}}) - \frac{1}{2} > 0.32492$. Therefore, in particular, the continuity of $\tilde{\boldsymbol{\varphi}}$ is established. ■

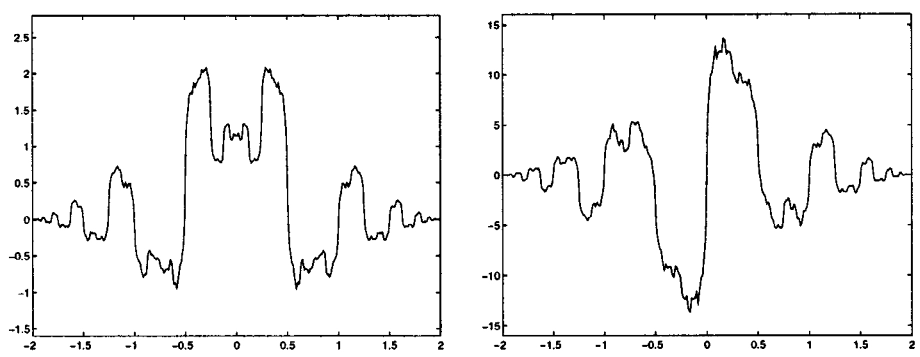

Fig. 2. Multigenerator $\tilde{\boldsymbol{\varphi}} = (\tilde{\varphi}_1, \tilde{\varphi}_2)^T$ on $\mathbb{R}$.

Clearly we have here that supp $\tilde{\varphi} = [-2, 2]$ is larger than supp φ. Note that $\tilde{\mathbf{A}}$ is also symmetric in the sense of (2.8). From this, it follows that the entry $\tilde{\varphi}_1$ of the multigenerator $\tilde{\varphi}$ is symmetric while $\tilde{\varphi}_2$ is antisymmetric around 0 [JRZ2], see Figure 2.

3.2. *Polynomial Exactness*

We call the multigenerator φ *exact of order* d (or say that φ has *accuracy* d) if all polynomials of degree at most $d-1$ can be written as a linear combination of the $\varphi_i(\cdot - k)$. As in [DKU1], the exactness will be used in Section 4 to derive multigenerators on the interval with properties (I)–(IV).

Polynomial exactness of refinable vectors of functions was discussed in [HSS], [JRZ1], and [P]. In [J, Theorem 4.1], a characterization for the accuracy of $\tilde{\varphi}$ was given in a form slightly different from that of [HSS]. Although the result is not new, it is convenient for applications. We briefly recall the main facts, specialized to the case at hand. The relations (3.2.6) and (3.2.9) below could also be derived by hand using polynomial exactness and biorthogonality. However, just applying the following proposition yields all the desired relations without tedious calculations:

Proposition 3.3. *Let* $\mathbf{f} = (f_1, f_2)^T$ *be a vector of compactly supported distributions. Suppose* $\mathbf{f}$ *satisfies the vector refinement equation* $\mathbf{f} = \sum_{k\in\mathbb{Z}} \mathbf{F}_k \mathbf{f}(2\cdot - k)$, *where each* $\mathbf{F}_k$ *is a* 2×2 *complex matrix. For* $m = 0, 1, 2, \ldots,$ *set*

$$\mathbf{E}_m := \frac{1}{m!}\sum_{k\in\mathbb{Z}}(2k)^m \mathbf{F}_{2k} \qquad \textit{and} \qquad \mathbf{O}_m := \frac{1}{m!}\sum_{k\in\mathbb{Z}}(2k-1)^m \mathbf{F}_{2k-1}. \tag{3.2.1}$$

Let d be a positive integer. If there exist vectors $\mathbf{y}_m \in \mathbb{R}^2$ *for* $m = 0, 1, \ldots, d-1$ *such that*

$$\sum_{m=0}^{r}(-1)^m 2^{r-m}\mathbf{y}_{r-m}^T \mathbf{E}_m = \mathbf{y}_r^T \qquad \textit{and} \qquad \sum_{m=0}^{r}(-1)^m 2^{r-m}\mathbf{y}_{r-m}^T \mathbf{O}_m = \mathbf{y}_r^T \tag{3.2.2}$$

are true for $r = 0, 1, \ldots, d-1$, *and if* $\mathbf{y}_0 \neq \mathbf{0}$, *then* $\mathbf{f}$ *has accuracy* d. *Moreover, under the condition* $\mathbf{y}_0^T \hat{\mathbf{f}}(0) = 1$, *we have*

$$\frac{x^r}{r!} = \sum_{k\in\mathbb{Z}}\sum_{m=0}^{r}\frac{k^m}{m!}\mathbf{y}_{r-m}^T \mathbf{f}(x-k), \qquad x \in \mathbb{R}, \quad r = 0, 1, \ldots, d-1. \tag{3.2.3}$$

Conversely, if $\mathbf{f}$ *is exact of order* d *and if the shifts of* f_1, f_2 *are linearly independent, then there exist vectors* $\mathbf{y}_m \in \mathbb{R}^2$, $m = 0, 1, \ldots, d-1$, *satisfying* $\mathbf{y}_0 \neq \mathbf{0}$ *and the conditions in* (3.2.2).

In fact, the above result remains valid if the sequences $(\hat{f}_i(\xi + 2k\pi))_{k\in\mathbb{Z}}$, $i = 1, 2$, are linearly independent for $\xi = 0$ and $\xi = \pi$. Here $\hat{f}$ denotes as usual the Fourier transform of f.

Applying the criterion in Proposition 3.3 to the vector φ of Hermite cubic splines, we obtain

$$\mathbf{y}_0 = \begin{bmatrix}1\\0\end{bmatrix}, \qquad \mathbf{y}_1 = \begin{bmatrix}0\\1\end{bmatrix}, \qquad \mathbf{y}_2 = \begin{bmatrix}0\\0\end{bmatrix}, \qquad \mathbf{y}_3 = \begin{bmatrix}0\\0\end{bmatrix}.$$

Defining the (column) vector

$$\tilde{\boldsymbol{\alpha}}_{k,r} := \int_{\mathbb{R}} x^r \tilde{\boldsymbol{\varphi}}(x-k)\,dx := \begin{bmatrix} \int_{\mathbb{R}} x^r \tilde{\varphi}_1(x-k)\,dx \\ \int_{\mathbb{R}} x^r \tilde{\varphi}_2(x-k)\,dx \end{bmatrix} \in \mathbb{R}^2, \tag{3.2.4}$$

one has then, also in view of (3.1), for $r = 0, \ldots, 3$,

$$x^r = \sum_{k\in\mathbb{Z}} \tilde{\boldsymbol{\alpha}}_{k,r}^T \boldsymbol{\varphi}(x-k) := \sum_{k\in\mathbb{Z}} \sum_{i=1}^{2} (\tilde{\boldsymbol{\alpha}}_{k,r})_i \varphi_i(x-k), \tag{3.2.5}$$

i.e., the Hermite cubics have exactness of order $d = 4$. These results can also be derived from the interpolation properties of the Hermite cubics. Applying the criterion in Proposition 3.3 to the vector $\boldsymbol{\varphi}$ of Hermite cubic splines, from (3.2.3), we have

$$x^r = \sum_{k\in\mathbb{Z}} \left[\sum_{m=0}^{r} \frac{r!\,k^m}{m!} \mathbf{y}_{r-m}^T \right] \boldsymbol{\varphi}(x-k), \qquad r = 0, \ldots, 3.$$

For all $k \in \mathbb{Z}$, comparing the above equality with (3.2.5), we obtain

$$\tilde{\boldsymbol{\alpha}}_{k,0} = \begin{bmatrix} 1 \\ 0 \end{bmatrix}, \qquad \tilde{\boldsymbol{\alpha}}_{k,1} = \begin{bmatrix} k \\ 1 \end{bmatrix}, \qquad \tilde{\boldsymbol{\alpha}}_{k,2} = \begin{bmatrix} k^2 \\ 2k \end{bmatrix}, \qquad \tilde{\boldsymbol{\alpha}}_{k,3} = \begin{bmatrix} k^3 \\ 3k^2 \end{bmatrix}. \tag{3.2.6}$$

Specifically, for $r = 0$ and $x = 0$, it follows from (2.2) and (3.1) that

$$\int_{\mathbb{R}} \tilde{\boldsymbol{\varphi}}(x)\,dx = \begin{bmatrix} 1 \\ 0 \end{bmatrix} = \int_{\mathbb{R}} \boldsymbol{\varphi}(x)\,dx. \tag{3.2.7}$$

Furthermore, we get:

Proposition 3.4. *The dual multigenerator $\tilde{\boldsymbol{\varphi}}$ is exact of order $\tilde{d} = 2$, i.e., for $r = 0, 1$ one has*

$$x^r = \sum_{k\in\mathbb{Z}} \boldsymbol{\alpha}_{k,r}^T \tilde{\boldsymbol{\varphi}}(x-k), \tag{3.2.8}$$

where for all $k \in \mathbb{Z}$

$$\boldsymbol{\alpha}_{k,r} := \int_{\mathbb{R}} x^r \boldsymbol{\varphi}(x-k)\,dx = \begin{cases} \begin{bmatrix} 1 \\ 0 \end{bmatrix}, & r = 0, \\[2ex] \begin{bmatrix} k \\ \frac{1}{15} \end{bmatrix}, & r = 1. \end{cases} \tag{3.2.9}$$

Proof. We apply the criterion in Proposition 3.3 to the dual vector $\tilde{\boldsymbol{\varphi}}$ with the mask given by (3.4). In this case, we have

$$\mathbf{E}_0 = \begin{bmatrix} 1 & 0 \\ 0 & \frac{91}{32} \end{bmatrix}, \qquad \mathbf{O}_0 = \begin{bmatrix} 1 & 0 \\ 0 & -\frac{37}{16} \end{bmatrix}, \quad \mathbf{E}_1 = \begin{bmatrix} 0 & \frac{5}{16} \\ -\frac{87}{32} & 0 \end{bmatrix}, \qquad \mathbf{O}_1 = \begin{bmatrix} 0 & -\frac{3}{8} \\ \frac{99}{16} & 0 \end{bmatrix}.$$

For $r = 0, 1$, the equations in (3.2.2) become

$$\mathbf{y}_0^T \mathbf{E}_0 = \mathbf{y}_0^T, \qquad \mathbf{y}_0^T \mathbf{O}_0 = \mathbf{y}_0^T,$$

and

$$2\mathbf{y}_1^T \mathbf{E}_0 - \mathbf{y}_0^T \mathbf{E}_1 = \mathbf{y}_1^T, \qquad 2\mathbf{y}_1^T \mathbf{O}_0 - \mathbf{y}_0^T \mathbf{O}_1 = \mathbf{y}_1^T.$$

We find that $\mathbf{y}_0 = [1, 0]^T$ and $\mathbf{y}_1 = [0, \frac{1}{15}]^T$ satisfy the above equations. Moreover, $\mathbf{y}_0^T \hat{\tilde{\varphi}}(0) = 1$. Thus, from Proposition 3.3, by a similar argument as in (3.2.6), we get (3.2.9). ■

Note that by [JRZ1, Theorem 2.1], $\tilde{\varphi}$ does not reproduce polynomials of order 3.

The coefficients (3.2.6), (3.2.9) will be used below to define the multigenerators on [0, 1]. They can also be computed directly by means of recursion formulas as, e.g., in [DKU1]. This derivation only uses (3.2.7) and the refinement equations (3.2) or (2.4).

The compact support of φ, $\tilde{\varphi}$ and the duality condition (3.1) guarantee that the integer translates $\{\tilde{\varphi}_i(\cdot - k),\ k \in \mathbb{Z},\ i = 1, 2\}$ form an L_2-stable basis for their span $\tilde{S}_0$ in the sense of (2.3) [DKU1] so that we can denote $\tilde{\varphi}$ as multigenerator *dual* to φ or simply *dual multigenerator*.

To distinguish shift-invariant quantities from analogs defined on an interval, it is convenient to write for the vector field $\mathbf{g}\colon\ \mathbb{R} \to \mathbb{R}^2$

$$\mathbf{g}_{[j,k]} = 2^{j/2}\mathbf{g}(2^j \cdot -k) := \begin{bmatrix} 2^{j/2}g_1(2^j \cdot -k) \\ 2^{j/2}g_2(2^j \cdot -k) \end{bmatrix}, \qquad j, k \in \mathbb{Z}.$$

In this notation, one can rewrite the refinement equation (2.4) in the form

$$\varphi_{[j,k]} = 2^{-1/2} \sum_{m=2k-1}^{2k+1} \mathbf{A}_{m-2k}\varphi_{[j+1,m]}. \tag{3.2.10}$$

The spaces

$$S_j := \operatorname{clos}_{L_2}(\operatorname{span}\{(\varphi_{[j,k]})_i, k \in \mathbb{Z}, i = 1, 2\})$$

and

$$\tilde{S}_j = \operatorname{clos}_{L_2}(\operatorname{span}\{(\tilde{\varphi}_{[j,k]})_i, k \in \mathbb{Z}, i = 1, 2\})$$

are, by the previous results, refinable and, thus, both form a hierarchy of nested spaces whose closure is dense in $L_2(\mathbb{R})$ and whose intersection consists only of 0. Hence, φ, $\tilde{\varphi}$ are *multigenerators* of the *primal* and *dual multiresolution sequences* $\mathcal{S} = \{S_j\}$, $\tilde{\mathcal{S}} = \{\tilde{S}_j\}$, see [JS].

Our next objective is to construct a pair of primal and dual multiresolution sequences on the interval [0, 1].

4. Multigenerators on [0, 1]

4.1. *Boundary Near Functions*

The strategy in [DKU1] is to use possibly many translates of the generators supported inside the interval and, in addition, to build fixed linear combinations of all generators overlapping the boundaries on the primal *and* on the dual sides such that polynomials up to the order of exactness are reproduced. On one hand, this allows us, in spite of the different sizes of support, to match the cardinality of the primal and dual multigenerator bases on the interval. On the other hand, as pointed out below, the resulting multiresolution spaces inherit the approximation properties of those defined on $\mathbb{R}$.

The construction will be carried out on one *fixed* level $j = j_0$. For the minimal level $j_0 := 3$, the modified functions at the left and at the right boundary do not overlap so that each end of the interval can be treated separately. It will be seen that for all levels $j \geq j_0$ the boundary modifications will be the same.

Suppose that $\varphi, \tilde{\varphi}$ form a dual pair of multigenerators as in Section 3 with φ from Section 2 having support $[-1, 1]$ and which is exact of order 4. We first define sets of indices on the primal and dual sides which have equal cardinality so that their interior functions are supported in $[0, 1]$. Since supp $\tilde{\varphi} = [-2, 2] \supset$ supp φ, let

$$\tilde{\Delta}_j^I := \{2, \dots, 2^j - 2\} \tag{4.1.1}$$

so that

$$\operatorname{supp} \tilde{\varphi}_{[j,k]} \subset [0, 1], \qquad k \in \tilde{\Delta}_j^I. \tag{4.1.2}$$

Note that $\#\tilde{\Delta}_j^I = 2^j - 3$ but since $\tilde{\varphi} \in \mathbb{R}^2$, every index stands in fact for two functions $(\tilde{\varphi}_1)_{[j,k]}, (\tilde{\varphi}_2)_{[j,k]}$. It will be useful to define the corresponding boundary index sets $\tilde{\Delta}_j^L, \tilde{\Delta}_j^R$

$$\tilde{\Delta}_j^L := \{1\}, \qquad \tilde{\Delta}_j^R := \{2^j - 1\}, \tag{4.1.3}$$

whose indices will again represent two (= order of exactness of $\tilde{\varphi}$) boundary functions each. We then have to define the appropriate index sets on the primal side, $\Delta_j^L, \Delta_j^I, \Delta_j^R$, such that the cardinality of the two sets

$$\tilde{\Delta}_j := \tilde{\Delta}_j^L \cup \tilde{\Delta}_j^I \cup \tilde{\Delta}_j^R, \qquad \Delta_j := \Delta_j^L \cup \Delta_j^I \cup \Delta_j^R, \tag{4.1.4}$$

is equal, and such that $\#\Delta_j^X = 2$ (= $\frac{1}{2}$ order of exactness of φ), $X \in \{L, R\}$, and supp $\varphi_{[j,k]} \subset [0, 1]$ for $k \in \Delta_j^I$. These requirements are satisfied when taking

$$\Delta_j^L := \{1, 2\}, \qquad \Delta_j^I := \{3, \dots, 2^j - 3\}, \qquad \Delta_j^R := \{2^j - 2, 2^j - 1\}, \tag{4.1.5}$$

see Figure 3.

We now define the boundary near functions at the left boundary by

$$\eta_{j,r}^L(x) := \sum_{m=0}^{2} \tilde{\boldsymbol{\alpha}}_{m,r}^T \varphi_{[j,m]}(x)|_{[0,1]}, \qquad r = 0, \dots, 3, \tag{4.1.6}$$

which we assemble for convenience in the boundary vectors

$$\varphi_{j,1}^{L,\vee} := \begin{bmatrix} \eta_{j,0}^L \\ \eta_{j,1}^L \end{bmatrix}, \qquad \varphi_{j,2}^{L,\vee} := \begin{bmatrix} \eta_{j,2}^L \\ \eta_{j,3}^L \end{bmatrix}. \tag{4.1.7}$$

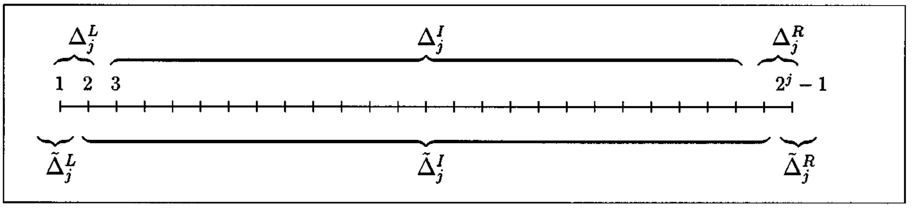

Fig. 3. Index sets for the interval: each index corresponds to a two-dimensional vector of functions.

On the dual side, let

$$\tilde{\eta}^L_{j,r}(x) := \sum_{m=-1}^{1} \boldsymbol{\alpha}^T_{m,r}\tilde{\boldsymbol{\varphi}}_{[j,m]}(x)|_{[0,1]}, \qquad r = 0, 1, \tag{4.1.8}$$

and, correspondingly,

$$\tilde{\boldsymbol{\varphi}}^{L,\vee}_{j,1} := \begin{bmatrix} \tilde{\eta}^L_{j,0} \\ \tilde{\eta}^L_{j,1} \end{bmatrix}. \tag{4.1.9}$$

In order to make the most out of symmetry when defining the boundary near functions at the right interval end, note that, by (2.6),

$$\begin{aligned} \boldsymbol{\varphi}_{[j,k]}(1-x) &= \mathbf{J}\boldsymbol{\varphi}_{[j,2^j-k]}(x), \\ \tilde{\boldsymbol{\varphi}}_{[j,k]}(1-x) &= \mathbf{J}\tilde{\boldsymbol{\varphi}}_{[j,2^j-k]}(x), \qquad x \in \mathbb{R}, \quad k \in \mathbb{Z}, \end{aligned} \tag{4.1.10}$$

with $\mathbf{J}$ defined in (2.7) and

$$\begin{aligned} \tilde{\boldsymbol{\alpha}}^R_{j,m,r} &:= -\int_{\mathbb{R}} (2^j - x)^r\, \tilde{\boldsymbol{\varphi}}(x-m)\, dx = \mathbf{J}\tilde{\boldsymbol{\alpha}}_{2^j-m,r}, \\ \boldsymbol{\alpha}^R_{j,m,r} &:= -\int_{\mathbb{R}} (2^j - x)^r\, \boldsymbol{\varphi}(x-m)\, dx = \mathbf{J}\boldsymbol{\alpha}_{2^j-m,r}. \end{aligned} \tag{4.1.11}$$

Defining, at the right boundary, $\eta_{j,2^j-r}$, $\tilde{\eta}_{j,2^j-r}$ in an analogous fashion by replacing x^r by $(1-x)^r$ and $\tilde{\boldsymbol{\alpha}}_{m,r}$ by $\tilde{\boldsymbol{\alpha}}^R_{j,m,r}$ and finally $\boldsymbol{\alpha}_{m,r}$ by $\boldsymbol{\alpha}^R_{j,m,r}$,

$$\eta^R_{j,2^j-r}(x) := \sum_{m=2^j-2}^{2^j} (\tilde{\boldsymbol{\alpha}}^R_{j,m,r})^T \boldsymbol{\varphi}_{[j,m]}(x)|_{[0,1]}, \qquad r = 0, \ldots, 3, \tag{4.1.12}$$

and

$$\tilde{\eta}^R_{j,2^j-r}(x) := \sum_{m=2^j-1}^{2^j+1} (\boldsymbol{\alpha}^R_{j,m,r})^T \tilde{\boldsymbol{\varphi}}_{[j,m]}(x)|_{[0,1]}, \qquad r = 0, 1, \tag{4.1.13}$$

one can then immediately, on account of (4.1.11), (4.1.10), and $\mathbf{J}^2 = \mathbf{I}$, establish the symmetry relations

$$\begin{aligned} \eta^R_{j,2^j-r}(1-x) &= \sum_{m=2^j-2}^{2^j} \tilde{\boldsymbol{\alpha}}^T_{2^j-m,r}\mathbf{J}\boldsymbol{\varphi}_{[j,m]}(1-x)|_{[0,1]} \\ &= \eta^L_{j,r}(x), \qquad r = 0, \ldots, 3, \quad x \in [0, 1], \end{aligned} \tag{4.1.14}$$

and

$$\tilde{\eta}^R_{j,2^j-r}(1-x) = \tilde{\eta}^L_{j,r}(x), \qquad r = 0, 1, \quad x \in [0, 1]. \tag{4.1.15}$$

We also assemble the functions at the right boundary in the two-dimensional vectors

$$\boldsymbol{\varphi}^{R,\vee}_{j,2^j-2} := \begin{bmatrix} \eta^R_{j,2^j-3} \\ \eta^R_{j,2^j-2} \end{bmatrix}, \quad \boldsymbol{\varphi}^{R,\vee}_{j,2^j-1} := \begin{bmatrix} \eta^R_{j,2^j-1} \\ \eta^R_{j,2^j} \end{bmatrix}, \quad \tilde{\boldsymbol{\varphi}}^{R,\vee}_{j,2^j-1} := \begin{bmatrix} \tilde{\eta}^R_{j,2^j-1} \\ \tilde{\eta}^R_{j,2^j} \end{bmatrix}. \tag{4.1.16}$$

Remark 4.1. By definition, the set

$$\Phi_j^{\vee} := \Phi_j^{L,\vee} \cup \Phi_j^{I} \cup \Phi_j^{R,\vee}, \tag{4.1.17}$$

where

$$\begin{aligned} \Phi_j^{L,\vee} &:= \{\varphi_{j,k}^{L,\vee}, k = 1, 2\}, \\ \Phi_j^{I} &:= \{\varphi_{[j,k]}, k \in \Delta_j^I\} = \{\varphi_{j,k}, k \in \Delta_j^I\}, \\ \Phi_j^{R,\vee} &:= \{\varphi_{j,2^j-k}^{R,\vee},\ k = 2, 1\}, \end{aligned} \tag{4.1.18}$$

still reproduces all polynomials of degree 3 on [0, 1]. Correspondingly, the set

$$\tilde{\Phi}_j^{\vee} := \tilde{\varphi}_j^{L,\vee} \cup \tilde{\varphi}_j^{I,\vee} \cup \tilde{\varphi}_j^{R,\vee}, \tag{4.1.19}$$

defined as

$$\tilde{\Phi}_j^{L,\vee} := \{\tilde{\varphi}_{j,1}^{L,\vee}\}, \qquad \tilde{\Phi}_j^{I,\vee} := \{\tilde{\varphi}_{[j,k]}, k \in \tilde{\Delta}_j^I\}, \qquad \tilde{\Phi}_j^{R,\vee} := \{\tilde{\varphi}_{j,2^j-1}^{R,\vee}\}, \tag{4.1.20}$$

reproduces by construction all linear polynomials on [0,1].

In the sequel, we will use both the interpretation of $\Phi_j^{\vee}$, etc., as a collection of functions (4.1.17), or as a (column) vector of functions containing all the functions in its set in the obvious order.

We have employed here the additional notation "$^{\vee}$" to indicate that these functions are still preliminary and will have to be modified.

4.2. *Refinability of Boundary Near Functions*

We next derive refinement equations for the boundary near functions (4.1.6), (4.1.8). For their right-end counterparts, one can use symmetry.

Suppose that $\boldsymbol{\theta}, \tilde{\boldsymbol{\theta}}$ form a pair of dual refinable multigenerators, as in Section 3, with $\operatorname{supp} \boldsymbol{\theta} = [-\lambda, \lambda]$, and that $\boldsymbol{\theta}$ is exact of order d. Let $\mathbf{A} = \{\mathbf{A}_k\}_{k=-\lambda}^{\lambda}$ denote the mask of $\boldsymbol{\theta}$ satisfying $\mathbf{A}_k := \mathbf{0}$ for $k < -\lambda$ or $k > \lambda$.

Lemma 4.2. *Let $\ell \geq \lambda$ and define*

$$\vartheta_{j,r}^{L} := \sum_{m=-\lambda+1}^{\ell-1} \boldsymbol{\alpha}_{\tilde{\boldsymbol{\theta}},r}(m)^T \boldsymbol{\theta}_{[j,m]}|_{\mathbb{R}_+}, \qquad r = 0, \dots, d-1, \tag{4.2.1}$$

where

$$\boldsymbol{\alpha}_{\tilde{\boldsymbol{\theta}},r}(m) := \int_{\mathbb{R}} x^r\, \tilde{\boldsymbol{\theta}}(x-m)\, dx. \tag{4.2.2}$$

Then one has

$$\begin{aligned} \vartheta_{j,r}^{L} \;=\; & 2^{-(r+1/2)} \left(\vartheta_{j+1,r}^{L} + \sum_{m=\ell}^{2\ell-\lambda-1} \boldsymbol{\alpha}_{\tilde{\boldsymbol{\theta}},r}(m)^T \boldsymbol{\theta}_{[j+1,m]} \right) \\ & + \sum_{m=2\ell-\lambda}^{2\ell+\lambda-2} \boldsymbol{\beta}_{\tilde{\boldsymbol{\theta}},r}(m)^T \boldsymbol{\theta}_{[j+1,m]}, \qquad r = 0, \dots, d-1, \end{aligned} \tag{4.2.3}$$

where

$$\beta_{\tilde{\theta},r}(m)^T := 2^{-1/2} \sum_{q=\lceil (m-\lambda)/2 \rceil}^{\ell-1} \alpha_{\tilde{\theta},r}(q)^T \mathbf{A}_{m-2q} \tag{4.2.4}$$

and $\lfloor x \rfloor$ ($\lceil x \rceil$) *is the largest* (*smallest*) *integer less* (*greater*) *than or equal to* x.

To verify the above relations, one can apply arguments following the lines in the proof of Lemma 3.1 in [DKU1].

4.3. *Basis Transformations and Biorthogonalization*

Although the construction of the boundary near functions in (4.1.17) and (4.1.19) preserves the exactness of the primal and dual multiresolutions:

(A) the functions in $\Phi_j^{L,\vee}$ and $\Phi_j^{R,\vee}$ no longer interpolate function values and first derivatives;
(B) $\Phi_j^\vee$ and $\tilde{\Phi}_j^\vee$ are not biorthogonal with respect to $(\cdot,\cdot)_{[0,1]}$.

Both shortcomings can be remedied by applying linear transformations to the boundary near functions.

To tackle (A), first recall that $\varphi_{[j,k]}$ is interpolating at $2^{-j}k$ with values

$$\varphi_{[j,k]}(2^{-j}m) = \delta_{k,m}\, 2^{j/2} \begin{bmatrix} 1 \\ 0 \end{bmatrix}, \quad \varphi'_{[j,k]}(2^{-j}m) = \delta_{k,m}\, 2^{3j/2} \begin{bmatrix} 0 \\ 1 \end{bmatrix}, \quad k,m \in \mathbb{Z}. \tag{4.3.1}$$

Thus, define $\mathbf{C}_L \in \mathbb{R}^{4\times 4}$ ($4 =$ order of exactness of φ) such that the new boundary functions

$$\Phi_j^L := \mathbf{C}_L \Phi_j^{L,\vee} \tag{4.3.2}$$

satisfy

(4.3.3)
$$\varphi_{j,1}^L(0) =: \varphi_{j,1}(0) = 2^{j/2} \begin{bmatrix} 1 \\ 0 \end{bmatrix}, \qquad (\varphi_{j,1}^L)'(0) =: (\varphi_{j,1})'(0) = 2^{3j/2} \begin{bmatrix} 0 \\ 1 \end{bmatrix},$$
$$\varphi_{j,2}^L(2^{-j}) =: \varphi_{j,2}(2^{-j}) = 2^{j/2} \begin{bmatrix} 1 \\ 0 \end{bmatrix}, \qquad (\varphi_{j,2}^L)'(2^{-j}) =: (\varphi_{j,2})'(2^{-j}) = 2^{3j/2} \begin{bmatrix} 0 \\ 1 \end{bmatrix},$$

and

$$\varphi_{j,1}(2^{-j}k) = (\varphi_{j,1})'(2^{-j}k) = \begin{bmatrix} 0 \\ 0 \end{bmatrix}, \qquad k \in \Delta_j^I \cup \{1, 2^j - 1\},$$
$$\varphi_{j,2}(2^{-j}k) = (\varphi_{j,2})'(2^{-j}k) = \begin{bmatrix} 0 \\ 0 \end{bmatrix}, \qquad k \in \Delta_j^I \cup \{0, 2^j\}.$$

Although this choice suggests itself, one could, of course, also define Φ_j^L such that $\varphi_{j,1}, \varphi_{j,2}$ interpolate at 2^{-j} and $2 \cdot 2^{-j}$ instead of at 0 and 2^{-j}.

Inserting the conditions (4.3.3), we have on the left-hand side of (4.3.2) the 4×4 matrix

(4.3.4) $$[\Phi_j^L(0), (\Phi_j^L)'(0), \Phi_j^L(2^{-j}), (\Phi_j^L)'(2^{-j})] = 2^{j/2}\begin{bmatrix} 1 & 0 & 0 & 0 \\ 0 & 2^j & 0 & 0 \\ 0 & 0 & 1 & 0 \\ 0 & 0 & 0 & 2^j \end{bmatrix}.$$

Using the values for $\tilde{\alpha}_{m,r}$ from (3.2.6), and (4.3.1), we can explicitly determine

(4.3.5) $$[\Phi_j^{L,\vee}(0), (\Phi_j^{L,\vee})'(0), \Phi_j^{L,\vee}(2^{-j}), (\Phi_j^{L,\vee})'(2^{-j})] = 2^{j/2}\begin{bmatrix} 1 & 0 & 1 & 0 \\ 0 & 2^j & 1 & 2^j \\ 0 & 0 & 1 & 2(2^j) \\ 0 & 0 & 1 & 3(2^j) \end{bmatrix}.$$

Thus, we obtain

(4.3.6) $$\mathbf{C}_L = \begin{bmatrix} 1 & 0 & -3 & 2 \\ 0 & 1 & -2 & 1 \\ 0 & 0 & 3 & -2 \\ 0 & 0 & -1 & 1 \end{bmatrix}, \qquad \mathbf{C}_L^{-1} = \begin{bmatrix} 1 & 0 & 1 & 0 \\ 0 & 1 & 1 & 1 \\ 0 & 0 & 1 & 2 \\ 0 & 0 & 1 & 3 \end{bmatrix}.$$

Note that the transformation $\mathbf{C}_L$ is independent of j. Furthermore, we obtain

(4.3.7) $$\Phi_j^{L,\vee}\left(\frac{2}{2^j}\right) = \Phi_j^{R,\vee}\left(1 - \frac{2}{2^j}\right) = 2^{j/2}\begin{bmatrix} 1 \\ 2 \\ 4 \\ 8 \end{bmatrix},$$
$$(\Phi_j^{L,\vee})'\left(\frac{2}{2^j}\right) = (\Phi_j^{R,\vee})'\left(1 - \frac{2}{2^j}\right) = 2^{3j/2}\begin{bmatrix} 0 \\ 1 \\ 4 \\ 12 \end{bmatrix}.$$

Denoting for any matrix $\mathbf{E}$ by $\mathbf{E}^\updownarrow$ the matrix which is obtained by reversing the order of rows and columns of $\mathbf{E}$, we define correspondingly at the right end of the interval

(4.3.8) $$\Phi_j^R := \mathbf{C}_R \Phi_j^{R,\vee}, \qquad \mathbf{C}_R := \mathbf{C}_L^\updownarrow,$$

so that $\varphi_{j,2^j-1} := \varphi_{j,2^j-1}^R$ interpolates function values and first derivatives at 1 and $\varphi_{j,2^j-2} := \varphi_{j,2^j-2}^R$ at $1 - 2^{-j}$. The inverse of $\mathbf{C}_R$ is determined as $\mathbf{C}_R^{-1} = (\mathbf{C}_L^{-1})^\updownarrow$.

Proposition 4.3. *The primal functions on the interval defined in* (4.3.2), (4.3.8),

(4.3.9) $$\Phi_j := \Phi_j^L \cup \Phi_j^I \cup \Phi_j^R$$

have the interpolation properties (4.3.3). *Moreover, except for the values* (4.3.7), *we have*

(4.3.10) $$\varphi_{j,k}(2^{-j}m) = \begin{bmatrix} 0 \\ 0 \end{bmatrix}, \qquad k \in \Delta_j, \quad m \in \Delta_j^I \cup \{0, 1, 2^j - 1, 2^j\}, \quad k \neq m.$$

To achieve (B) biorthogonality, we will apply another linear transformation, now on the dual boundary functions.

Let $\mathbf{I}^{(m)}$ denote the identity matrix of size m. Since changes have only been made to boundary near functions so that still

$$(\boldsymbol{\varphi}_{j,k}, \tilde{\boldsymbol{\varphi}}_{j,m})_{[0,1]} = \delta_{k,m}\mathbf{I}^{(2)}, \qquad k, m \in \Delta_j^I, \tag{4.3.11}$$

we only have to transform locally near the boundary. That is, we seek $\tilde{\mathbf{C}}_L \in \mathbb{R}^{4\times 4}$ such that the new dual boundary functions

$$\tilde{\Phi}_j^L := \tilde{\mathbf{C}}_L \tilde{\Phi}_j^{L,\vee} \tag{4.3.12}$$

satisfy

$$(\Phi_j^L, \tilde{\Phi}_j^L)_{[0,1]} = \mathbf{I}^{(4)}. \tag{4.3.13}$$

Here we have for simplicity also used the notation $\tilde{\Phi}_j^{L,\vee}$ for the functions $\{\tilde{\boldsymbol{\varphi}}_{j,1}^{L,\vee}, \tilde{\boldsymbol{\varphi}}_{[j,2]}\}$ in order to match the cardinality of Δ_j^L in (4.3.13).

Inserting (4.3.12) into (4.3.13), it follows that

$$\tilde{\mathbf{C}}_L = (\Phi_j^L, \tilde{\Phi}_j^{L,\vee})_{[0,1]}^{-T}. \tag{4.3.14}$$

Of course, one has to make sure that $(\Phi_j^L, \tilde{\Phi}_j^{L,\vee})_{[0,1]}$ is indeed invertible. In the following, we explicitly determine this matrix. Observe first that

$$\begin{aligned}(\boldsymbol{\varphi}_{j,1}, \tilde{\boldsymbol{\varphi}}_{j,1}^{L,\vee})_{[0,1]} &= \left(\boldsymbol{\varphi}_{j,1}, \begin{bmatrix} \sum_{m=-1}^{1} \boldsymbol{\alpha}_{m,0}^T \tilde{\boldsymbol{\varphi}}_{[j,m]} \\ \sum_{m=-1}^{1} \boldsymbol{\alpha}_{m,1}^T \tilde{\boldsymbol{\varphi}}_{[j,m]} \end{bmatrix}\right)_{[0,1]} \\ &= \left(\boldsymbol{\varphi}_{j,1}, \begin{bmatrix} \sum_{m=-1}^{\infty} \boldsymbol{\alpha}_{m,0}^T \tilde{\boldsymbol{\varphi}}_{[j,m]} \\ \sum_{m=-1}^{\infty} \boldsymbol{\alpha}_{m,1}^T \tilde{\boldsymbol{\varphi}}_{[j,m]} \end{bmatrix} - \begin{bmatrix} \boldsymbol{\alpha}_{2,0}^T \tilde{\boldsymbol{\varphi}}_{[j,2]} \\ \boldsymbol{\alpha}_{2,1}^T \tilde{\boldsymbol{\varphi}}_{[j,2]} \end{bmatrix}\right)_{[0,1]},\end{aligned} \tag{4.3.15}$$

since $\operatorname{supp} \tilde{\boldsymbol{\varphi}}_{[j,m]} \subset [0, \infty)$ for $m \geq 2$ and because of biorthogonality

$$(\boldsymbol{\varphi}_{[j,k]}, \tilde{\boldsymbol{\varphi}}_{[j,m]})_{\mathbb{R}} = \delta_{k,m}\mathbf{I}^{(2)}, \qquad k, m \in \mathbb{Z}. \tag{4.3.16}$$

Using for the first term on the right-hand side the fact that $\tilde{\boldsymbol{\varphi}}$ is exact of order 2 (3.2.8), we get

$$(\boldsymbol{\varphi}_{j,1}, \tilde{\boldsymbol{\varphi}}_{j,1}^{L,\vee})_{[0,1]} = \left(\boldsymbol{\varphi}_{j,1}, \begin{bmatrix} 2^{j/2} \\ 2^{j/2}(\cdot) \end{bmatrix} - \begin{bmatrix} \boldsymbol{\alpha}_{2,0}^T \tilde{\boldsymbol{\varphi}}_{[j,2]} \\ \boldsymbol{\alpha}_{2,1}^T \tilde{\boldsymbol{\varphi}}_{[j,2]} \end{bmatrix}\right)_{[0,1]}. \tag{4.3.17}$$

Substituting the definition of $\boldsymbol{\varphi}_{j,1}$ (4.3.2) with $\mathbf{C}_L$ given by (4.3.6), one obtains for the first term

$$\begin{aligned}&\left(\boldsymbol{\varphi}_{j,1}, \begin{bmatrix} 2^{j/2} \\ 2^{j/2}(\cdot) \end{bmatrix}\right)_{[0,1]} \\ &\quad= \begin{bmatrix} \sum_{m=0}^{2} (\tilde{\boldsymbol{\alpha}}_{m,0}^T - 3\tilde{\boldsymbol{\alpha}}_{m,2}^T + 2\tilde{\boldsymbol{\alpha}}_{m,3}^T) \\ \sum_{m=0}^{2} (\tilde{\boldsymbol{\alpha}}_{m,1}^T - 2\tilde{\boldsymbol{\alpha}}_{m,2}^T + \tilde{\boldsymbol{\alpha}}_{m,3}^T) \end{bmatrix} \left(\boldsymbol{\varphi}_{[j,m]}, \begin{bmatrix} 2^{j/2} \\ 2^{j/2}(\cdot) \end{bmatrix}\right)_{[0,1]} \\ &\quad= \begin{bmatrix} \sum_{m=0}^{2} (\tilde{\boldsymbol{\alpha}}_{m,0}^T - 3\tilde{\boldsymbol{\alpha}}_{m,2}^T + 2\tilde{\boldsymbol{\alpha}}_{m,3}^T) \\ \sum_{m=0}^{2} (\tilde{\boldsymbol{\alpha}}_{m,1}^T - 2\tilde{\boldsymbol{\alpha}}_{m,2}^T + \tilde{\boldsymbol{\alpha}}_{m,3}^T) \end{bmatrix} \left(\boldsymbol{\varphi}(\cdot - m), \begin{bmatrix} 1 \\ (\cdot) \end{bmatrix}\right)_{[0,\infty)}.\end{aligned} \tag{4.3.18}$$

Table 4.1. Values for $\int_0^\infty \varphi(x-m)x^r\,dx$, $r=0,1$, $m=0,1,2$.

$r\backslash m$	0	1	2
0	$\begin{bmatrix}\frac{1}{2}\\ \frac{1}{12}\end{bmatrix}$	$\begin{bmatrix}1\\ 0\end{bmatrix}$	$\begin{bmatrix}1\\ 0\end{bmatrix}$
1	$\begin{bmatrix}\frac{3}{20}\\ \frac{1}{30}\end{bmatrix}$	$\begin{bmatrix}1\\ \frac{1}{15}\end{bmatrix}$	$\begin{bmatrix}2\\ \frac{1}{15}\end{bmatrix}$

Using the explicit definition of φ (2.1), we can in turn compute the latter quantities on the right-hand side, see Table 4.1.

Together with the values for $\tilde{\alpha}_{m,r}$ from (3.2.6), the quantities (4.3.18) are therefore determined as

$$\left(\boldsymbol{\varphi}_{j,1}, \begin{bmatrix} 2^{j/2} \\ 2^{j/2}(\cdot) \end{bmatrix}\right)_{[0,1]} = \begin{bmatrix} \frac{11}{2} & \frac{219}{20} \\ \frac{25}{12} & \frac{131}{30} \end{bmatrix}. \tag{4.3.19}$$

For the second term in (4.3.17) we get, accordingly,

$$\left(\boldsymbol{\varphi}_{j,1}, \begin{bmatrix} \boldsymbol{\alpha}_{2,0}^T \tilde{\boldsymbol{\varphi}}_{[j,2]} \\ \boldsymbol{\alpha}_{2,1}^T \tilde{\boldsymbol{\varphi}}_{[j,2]} \end{bmatrix}\right)_{[0,1]} = \begin{bmatrix} 5 & \frac{54}{5} \\ 2 & \frac{13}{3} \end{bmatrix}. \tag{4.3.20}$$

Together, (4.3.19) and (4.3.20) yield

$$\left(\boldsymbol{\varphi}_{j,1}, \tilde{\boldsymbol{\varphi}}_{j,1}^{L,\vee}\right)_{[0,1]} = \begin{bmatrix} \frac{1}{2} & \frac{3}{20} \\ \frac{1}{12} & \frac{1}{30} \end{bmatrix}. \tag{4.3.21}$$

In the same fashion, we can compute

$$\left(\boldsymbol{\varphi}_{j,2}, \tilde{\boldsymbol{\varphi}}_{j,1}^{L,\vee}\right)_{[0,1]} = \begin{bmatrix} 1 & 1 \\ 0 & \frac{1}{15} \end{bmatrix}. \tag{4.3.22}$$

Moreover, since $\tilde{\boldsymbol{\varphi}}_{j,2}$ is already an interior function, we get

$$\begin{aligned} \left(\boldsymbol{\varphi}_{j,1}, \tilde{\boldsymbol{\varphi}}_{j,2}\right)_{[0,1]} &= \begin{bmatrix} \sum_{m=0}^{2}(\tilde{\boldsymbol{\alpha}}_{m,0}^T - 3\tilde{\boldsymbol{\alpha}}_{m,2}^T + 2\tilde{\boldsymbol{\alpha}}_{m,3}^T) \\ \sum_{m=0}^{2}(\tilde{\boldsymbol{\alpha}}_{m,1}^T - 2\tilde{\boldsymbol{\alpha}}_{m,2}^T + \tilde{\boldsymbol{\alpha}}_{m,3}^T) \end{bmatrix} (\boldsymbol{\varphi}(\cdot - m), \tilde{\boldsymbol{\varphi}}(\cdot - 2))_{\mathbb{R}} \\ &= \begin{bmatrix} \tilde{\boldsymbol{\alpha}}_{2,0}^T - 3\tilde{\boldsymbol{\alpha}}_{2,2}^T + 2\tilde{\boldsymbol{\alpha}}_{2,3}^T \\ \tilde{\boldsymbol{\alpha}}_{2,1}^T - 2\tilde{\boldsymbol{\alpha}}_{2,2}^T + \tilde{\boldsymbol{\alpha}}_{2,3}^T \end{bmatrix} = \begin{bmatrix} 5 & 12 \\ 2 & 5 \end{bmatrix} \end{aligned} \tag{4.3.23}$$

and

$$(\boldsymbol{\varphi}_{j,2}, \tilde{\boldsymbol{\varphi}}_{j,2})_{[0,1]} = \begin{bmatrix} -4 & -12 \\ 4 & 8 \end{bmatrix}. \tag{4.3.24}$$

Collecting the results (4.3.21), (4.3.22), (4.3.23), and (4.3.24), we obtain

$$(\Phi_j^L, \tilde{\Phi}_j^{L,\vee})_{[0,1]} = \begin{bmatrix} \frac{1}{2} & \frac{3}{20} & 5 & 12 \\ \frac{1}{12} & \frac{1}{30} & 2 & 5 \\ 1 & 1 & -4 & -12 \\ 0 & \frac{1}{15} & 4 & 8 \end{bmatrix},$$

which has determinant $\frac{16}{15} \neq 0$. By (4.3.14), this yields

$$\tilde{\mathbf{C}}_L = \begin{bmatrix} 4 & -5 & \frac{3}{4} & -\frac{1}{3} \\ -9 & 15 & -\frac{15}{4} & \frac{7}{4} \\ -\frac{1}{4} & \frac{5}{4} & -\frac{1}{16} & \frac{1}{48} \\ -\frac{3}{4} & 0 & \frac{9}{8} & -\frac{7}{16} \end{bmatrix}. \tag{4.3.25}$$

Corresponding to (4.3.12), we define at the right end of the interval

$$\tilde{\Phi}_j^R := \tilde{\mathbf{C}}_R \, \tilde{\Phi}_j^{R,\vee}, \tag{4.3.26}$$

where $\tilde{\mathbf{C}}_R$ is determined such that

$$(\Phi_j^R, \tilde{\Phi}_j^R)_{[0,1]} = \mathbf{I}^{(4)}, \tag{4.3.27}$$

i.e.,

$$\tilde{\mathbf{C}}_R = (\Phi_j^R, \tilde{\Phi}_j^{R,\vee})_{[0,1]}^{-T}. \tag{4.3.28}$$

Here $\tilde{\Phi}_j^{R,\vee}$ also denotes the set of functions $\{\tilde{\varphi}_{[j,2^j-2]}, \tilde{\varphi}_{j,2^j-1}^{R,\vee}\}$. Note that $\tilde{\mathbf{C}}_R$ cannot be obtained by simply reversing the rows and columns of $\tilde{\mathbf{C}}_L$ since $\tilde{\Phi}_j^{R,\vee} \neq (\tilde{\Phi}_j^{L,\vee})^{\updownarrow}$ because of the order of the interior functions. Thus, we will determine $\tilde{\mathbf{C}}_R$ explicitly by exploiting symmetry of the boundary near functions.

For the left upper block of $(\Phi_j^R, \tilde{\Phi}_j^{R,\vee})_{[0,1]}$, one obtains by (4.1.12), (4.3.2), (4.1.14), and (4.1.10)

$$\begin{aligned}
(\varphi_{j,2^j-2}, \tilde{\varphi}_{[j,2^j-2]})_{[0,1]} &= \left(\begin{bmatrix} \eta_{j,2^j-3}^R - \eta_{j,2^j-2}^R \\ -2\eta_{j,2^j-3}^R + 3\eta_{j,2^j-2}^R \end{bmatrix}, \tilde{\varphi}_{[j,2^j-2]} \right)_{[0,1]} \\
&= \left(\begin{bmatrix} \eta_{j,3}^L(1-\cdot) - \eta_{j,2}^L(1-\cdot) \\ -2\eta_{j,3}^L(1-\cdot) + 3\eta_{j,2}^L(1-\cdot) \end{bmatrix}, \mathbf{J}\tilde{\varphi}_{[j,2]}(1-\cdot) \right)_{[0,1]} \\
&= \left(\begin{bmatrix} \eta_{j,3}^L - \eta_{j,2}^L \\ -2\eta_{j,3}^L + 3\eta_{j,2}^L \end{bmatrix}, \tilde{\varphi}_{[j,2]} \right)_{[0,1]} \mathbf{J}.
\end{aligned}$$

Inserting the definitions we conclude, as in (4.3.23) and (4.3.24),

$$(\varphi_{j,2^j-2}, \tilde{\varphi}_{[j,2^j-2]})_{[0,1]} = \begin{bmatrix} 4 & -8 \\ -4 & 12 \end{bmatrix}. \tag{4.3.29}$$

Similarly, we derive the remainder of the entries so that we obtain we obtain

$$(\Phi_j^R, \tilde{\Phi}_j^{R,\vee})_{[0,1]} = \begin{bmatrix} 4 & -8 & \frac{1}{15} & 0 \\ -4 & 12 & 1 & 1 \\ 2 & -5 & \frac{1}{30} & \frac{1}{12} \\ 5 & -12 & \frac{3}{20} & \frac{1}{2} \end{bmatrix} \tag{4.3.30}$$

which also has determinant $\frac{16}{15} \neq 0$. By (4.3.28), this gives

$$\tilde{\mathbf{C}}_R = \begin{bmatrix} \frac{9}{8} & \frac{7}{16} & 0 & -\frac{3}{4} \\ -\frac{1}{16} & -\frac{1}{48} & \frac{5}{4} & -\frac{1}{4} \\ -\frac{15}{4} & -\frac{7}{4} & 15 & -9 \\ \frac{3}{4} & \frac{1}{3} & -5 & 4 \end{bmatrix}. \tag{4.3.31}$$

Proposition 4.4. *The dual functions on the interval defined in* (4.3.12), (4.3.26),

$$\tilde{\Phi}_j := \tilde{\Phi}_j^L \cup \tilde{\Phi}_j^I \cup \tilde{\Phi}_j^R, \tag{4.3.32}$$

where

$$\tilde{\Phi}_j^I := \left\{\tilde{\varphi}_{[j,k]}, k \in \Delta_j^I\right\} = \left\{\tilde{\varphi}_{j,k}, k \in \Delta_j^I\right\}, \tag{4.3.33}$$

satisfy, together with the Φ_j *given in* (4.3.9), *the biorthogonality conditions*

$$(\Phi_j, \tilde{\Phi}_j)_{[0,1]} = \mathbf{I}. \tag{4.3.34}$$

4.4. *Refinement Equations*

In this section, we derive from the previous sections the refinement relations for the biorthogonal generators Φ_j, $\tilde{\Phi}_j$. Since Φ_j, $\tilde{\Phi}_j$ can be interpreted as finite-dimensional vectors, the representation of such two-scale relations in *matrix–vector form* suggests itself.

According to Lemma 4.2, the first boundary adapted functions $\Phi_j^\vee$ defined in (4.1.17) satisfy the refinement equation

$$(\Phi_j^\vee)^T = (\Phi_{j+1}^\vee)^T \mathbf{M}_{j,0}^\vee \tag{4.4.1}$$

with

(4.4.2) $\mathbf{M}_{j,0}^\vee :=$

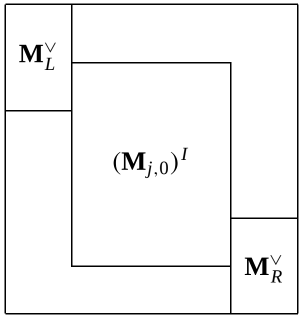

.

Table 4.2. Values of $\tilde{\boldsymbol{\beta}}_{5,r}$.

$5\backslash r$	0	1	2	3
5	$\begin{bmatrix} \frac{1}{2\sqrt{2}} \\ -\frac{3}{4\sqrt{2}} \end{bmatrix}$	$\begin{bmatrix} \frac{9}{8\sqrt{2}} \\ -\frac{13}{8\sqrt{2}} \end{bmatrix}$	$\begin{bmatrix} \frac{5}{2\sqrt{2}} \\ -\frac{7}{2\sqrt{2}} \end{bmatrix}$	$\begin{bmatrix} \frac{11}{2\sqrt{2}} \\ -\frac{15}{2\sqrt{2}} \end{bmatrix}$

In order to describe the block matrices used in (4.4.2), define according to (4.2.4)

$$\tilde{\boldsymbol{\beta}}_{5,r}^{T} := 2^{-1/2}\tilde{\boldsymbol{\alpha}}_{2,r}^{T}\mathbf{A}_1. \tag{4.4.3}$$

These values are computed in Table 4.2, the ones for the right-hand side defined as

$$(\boldsymbol{\beta}^{R}_{j,2^{j+1}-5,r})^{T} := 2^{-1/2}(\tilde{\boldsymbol{\alpha}}^{R}_{j,2^{j}-2,r})^{T}\mathbf{A}_{-1}\mathbf{J},$$

follow by symmetry $\tilde{\boldsymbol{\beta}}^{R}_{j,2^{j+1}-5,r} = \tilde{\boldsymbol{\beta}}_{5,r}$. The blocks $\mathbf{M}_L^{\vee}, \mathbf{M}_R^{\vee}$ in (4.4.2) are 10×4 matrices given then by

$$\mathbf{M}_L^{\vee} := \begin{bmatrix} 2^{-1/2} & & & \\ & 2^{-3/2} & & \\ & & 2^{-5/2} & \\ & & & 2^{-7/2} \\ 2^{-1/2}\tilde{\boldsymbol{\alpha}}_{3,0} & 2^{-3/2}\tilde{\boldsymbol{\alpha}}_{3,1} & 2^{-5/2}\tilde{\boldsymbol{\alpha}}_{3,2} & 2^{-7/2}\tilde{\boldsymbol{\alpha}}_{3,3} \\ 2^{-1/2}\tilde{\boldsymbol{\alpha}}_{4,0} & 2^{-3/2}\tilde{\boldsymbol{\alpha}}_{4,1} & 2^{-5/2}\tilde{\boldsymbol{\alpha}}_{4,2} & 2^{-7/2}\tilde{\boldsymbol{\alpha}}_{4,3} \\ \tilde{\boldsymbol{\beta}}_{5,0} & \tilde{\boldsymbol{\beta}}_{5,1} & \tilde{\boldsymbol{\beta}}_{5,2} & \tilde{\boldsymbol{\beta}}_{5,3} \end{bmatrix} =: \begin{bmatrix} \mathbf{D}_L \\ \mathbf{B}_L \end{bmatrix} \in \begin{cases} \mathbb{R}^{4\times 4}, \\ \mathbb{R}^{6\times 4}, \end{cases} \tag{4.4.4}$$

and

$$\mathbf{M}_R^{\vee} := \begin{bmatrix} \mathbf{J}\tilde{\boldsymbol{\beta}}^{R}_{j,2^{j+1}-5,3} & \mathbf{J}\tilde{\boldsymbol{\beta}}^{R}_{j,2^{j+1}-5,2} & \mathbf{J}\tilde{\boldsymbol{\beta}}^{R}_{j,2^{j+1}-5,1} & \mathbf{J}\tilde{\boldsymbol{\beta}}^{R}_{j,2^{j+1}-5,0} \\ 2^{-7/2}\tilde{\boldsymbol{\alpha}}^{R}_{2^{j+1}-4,3} & 2^{-5/2}\tilde{\boldsymbol{\alpha}}^{R}_{2^{j+1}-4,2} & 2^{-3/2}\tilde{\boldsymbol{\alpha}}^{R}_{2^{j+1}-4,1} & 2^{-1/2}\tilde{\boldsymbol{\alpha}}^{R}_{2^{j+1}-4,0} \\ 2^{-7/2}\tilde{\boldsymbol{\alpha}}^{R}_{2^{j+1}-3,3} & 2^{-5/2}\tilde{\boldsymbol{\alpha}}^{R}_{2^{j+1}-3,2} & 2^{-3/2}\tilde{\boldsymbol{\alpha}}^{R}_{2^{j+1}-3,1} & 2^{-1/2}\tilde{\boldsymbol{\alpha}}^{R}_{2^{j+1}-3,0} \\ 2^{-7/2} & & & \\ & 2^{-5/2} & & \\ & & 2^{-3/2} & \\ & & & 2^{-1/2} \end{bmatrix} \tag{4.4.5}$$

$$=: \begin{bmatrix} \mathbf{B}_R \\ \mathbf{D}_R \end{bmatrix} \in \begin{cases} \mathbb{R}^{6\times 4}, \\ \mathbb{R}^{4\times 4}. \end{cases}$$

Furthermore, the interior block $(\mathbf{M}^{\vee}_{j,0})^{I}$ in (4.4.2) is defined as

$$(\mathbf{M}_{j,0})^{I}_{m,k} := \frac{1}{\sqrt{2}}\mathbf{A}^{T}_{m-2k}, \qquad m \in \Delta^{I}_{j+1}, \quad k \in \Delta^{I}_{j}. \tag{4.4.6}$$

Note that only the *size* of $(\mathbf{M}_{j,0})^{I}$, not its band width nor its entries, depend on j.

Taking the transformation (4.3.2), to recover the interpolation conditions, into account, then yields that the Φ_j given by (4.3.9) satisfy a refinement equation with

(4.4.7) $\quad \mathbf{M}_{j,0} :=$

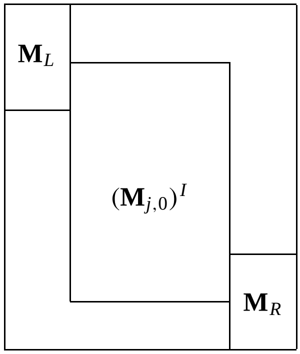

$= \mathbf{C}_{j+1}^{-T}\mathbf{M}_{j,0}^{\vee}\mathbf{C}_j^T,$

where

(4.4.8)
$$\mathbf{C}_j := \operatorname{diag}(\mathbf{C}_L, \mathbf{I}, \mathbf{C}_R)$$

with $\mathbf{C}_L$, $\mathbf{C}_R$ from (4.3.6), (4.3.8), see [DKU1]. In particular, $\mathbf{M}_L$, $\mathbf{M}_R$ have the form

(4.4.9)
$$\mathbf{M}_L = \begin{bmatrix} \mathbf{C}_L^{-T}\mathbf{D}_L\mathbf{C}_L^T \\ \mathbf{B}_L\mathbf{C}_L^T \end{bmatrix}, \qquad \mathbf{M}_R = \begin{bmatrix} \mathbf{B}_R\mathbf{C}_R^T \\ \mathbf{C}_R^{-T}\mathbf{D}_R\mathbf{C}_R^T \end{bmatrix}.$$

From (4.2.3), we infer that the dual initial functions $\tilde{\Phi}_j^{\vee}$ defined in (4.1.19) satisfy the refinement equation

(4.4.10)
$$(\tilde{\Phi}_j^{\vee})^T = (\tilde{\Phi}_{j+1}^{\vee})^T\tilde{\mathbf{M}}_{j,0}^{\vee}.$$

The structure of $\tilde{\mathbf{M}}_{j,0}^{\vee}$ is completely analogous to that of $\mathbf{M}_{j,0}^{\vee}$ illustrated in (4.4.2) with blocks $\tilde{\mathbf{M}}_L^{\vee}$, $(\tilde{\mathbf{M}}_{j,0})^I$, and $\tilde{\mathbf{M}}_R^{\vee}$. To give a detailed description of these blocks, define, according to (4.2.4),

$$\boldsymbol{\beta}_{s,r}^T := 2^{-1/2}\sum_{q=\lceil (s-2)/2\rceil}^{1}\boldsymbol{\alpha}_{q,r}^T\tilde{\mathbf{A}}_{s-2q}.$$

These values are computed in Table 4.3, the ones for the right end of the interval

$$(\boldsymbol{\beta}_{j,s,r}^R)^T := 2^{-1/2}\sum_{m=2^j-1}^{2^j-\lceil (s-2)/2\rceil}(\boldsymbol{\alpha}_{j,m,r}^R)^T\tilde{\mathbf{A}}_{2^{j+1}-2m-s}\mathbf{J}$$

follow again by symmetry $\boldsymbol{\beta}_{j,s,r}^R = \boldsymbol{\beta}_{2^{j+1}-s,r}$. The boundary blocks are now given by

(4.4.11)
$$\tilde{\mathbf{M}}_L^{\vee} := \begin{bmatrix} 2^{-1/2} & \\ & 2^{-3/2} \\ \boldsymbol{\beta}_{2,0} & \boldsymbol{\beta}_{2,1} \\ \boldsymbol{\beta}_{3,0} & \boldsymbol{\beta}_{3,1} \\ \boldsymbol{\beta}_{4,0} & \boldsymbol{\beta}_{4,1} \end{bmatrix} =: \begin{bmatrix} \tilde{\mathbf{D}}_L \\ \tilde{\mathbf{B}}_L \end{bmatrix} \in \begin{cases} \mathbb{R}^{2\times 2}, \\ \mathbb{R}^{6\times 2}, \end{cases}$$

Table 4.3

$r\backslash m$	2	3	4
0	$\begin{bmatrix} \frac{71}{64\sqrt{2}} \\ \frac{5}{64\sqrt{2}} \end{bmatrix}$	$\begin{bmatrix} \frac{1}{2\sqrt{2}} \\ -\frac{3}{16\sqrt{2}} \end{bmatrix}$	$\begin{bmatrix} -\frac{7}{64\sqrt{2}} \\ \frac{5}{64\sqrt{2}} \end{bmatrix}$
1	$\begin{bmatrix} \frac{2253}{128\cdot 15\sqrt{2}} \\ \frac{151}{64\cdot 15\sqrt{2}} \end{bmatrix}$	$\begin{bmatrix} \frac{339}{32\cdot 15\sqrt{2}} \\ -\frac{127}{32\cdot 15\sqrt{2}} \end{bmatrix}$	$\begin{bmatrix} -\frac{297}{128\cdot 15\sqrt{2}} \\ \frac{106}{64\cdot 15\sqrt{2}} \end{bmatrix}$

and

(4.4.12) $$\tilde{\mathbf{M}}_R^{\vee} := \begin{bmatrix} \mathbf{J}\boldsymbol{\beta}^R_{j,2^{j+1}-4,1} & \mathbf{J}\boldsymbol{\beta}^R_{j,2^{j+1}-4,0} \\ \mathbf{J}\boldsymbol{\beta}^R_{j,2^{j+1}-3,1} & \mathbf{J}\boldsymbol{\beta}^R_{j,2^{j+1}-3,0} \\ \mathbf{J}\boldsymbol{\beta}^R_{j,2^{j+1}-2,1} & \mathbf{J}\boldsymbol{\beta}^R_{j,2^{j+1}-2,0} \\ 2^{-3/2} & \\ & 2^{-1/2} \end{bmatrix} =: \begin{bmatrix} \tilde{\mathbf{B}}_R \\ \tilde{\mathbf{D}}_R \end{bmatrix} \in \begin{cases} \mathbb{R}^{6\times 2}, \\ \mathbb{R}^{2\times 2}. \end{cases}$$

Of course, the interior block $(\tilde{\mathbf{M}}^{\vee}_{j,0})^I$ is of the form

(4.4.13) $$(\tilde{\mathbf{M}}_{j,0})^I_{m,k} := \frac{1}{\sqrt{2}}\,\tilde{\mathbf{A}}^T_{m-2k}, \qquad m \in \tilde{\Delta}^I_{j+1}, \quad k \in \tilde{\Delta}^I_j,$$

where only its size depends on j. Considering the transformation which restores biorthogonality (4.3.12), we obtain that the final dual multigenerators $\tilde{\Phi}_j$ defined in (4.3.32) satisfy the refinement equation with

(4.4.14) $\tilde{\mathbf{M}}_{j,0} :=$

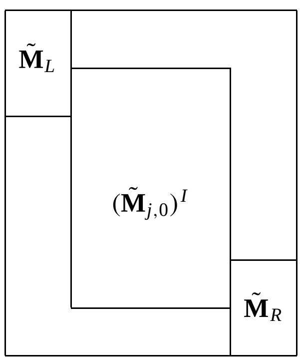

$= \tilde{\mathbf{C}}^{-T}_{j+1}\tilde{\mathbf{M}}^{\vee}_{j,0}\tilde{\mathbf{C}}^T_j,$

where

(4.4.15) $$\tilde{\mathbf{C}}_j := \operatorname{diag}(\tilde{\mathbf{C}}_L, \mathbf{I}, \tilde{\mathbf{C}}_R)$$

with $\tilde{\mathbf{C}}_L$ and $\tilde{\mathbf{C}}_R$ from (4.3.25) and (4.3.31). Note that since $\tilde{\mathbf{C}}_L$ and $\tilde{\mathbf{C}}_R$ are 4×4 matrices, $\tilde{\mathbf{M}}_L$, $\tilde{\mathbf{M}}_R$ are now of size 12×4.

To simplify notation, we abbreviate

$$S(\Phi_j) := \operatorname{span}\{(\varphi_{j,k})_i,\ k \in \Delta_j,\ i = 1, 2\},$$

and analogously $S(\tilde{\Phi}_j)$.

We can now summarize our findings as follows:

Proposition 4.5. *The multiresolution spaces are nested,*

$$S(\Phi_j) \subset S(\Phi_{j+1}), \qquad S(\tilde{\Phi}_j) \subset S(\tilde{\Phi}_{j+1}),$$

i.e., the biorthogonal multigenerators Φ_j and $\tilde{\Phi}_j$ given by (4.3.9) *and* (4.3.32) *satisfy the refinement equations*

$$\Phi_j^T = \Phi_{j+1}^T \mathbf{M}_{j,0}, \qquad \tilde{\Phi}_j^T = \tilde{\Phi}_{j+1}^T \tilde{\mathbf{M}}_{j,0}, \tag{4.4.16}$$

with $\mathbf{M}_{j,0}$, $\tilde{\mathbf{M}}_{j,0}$ defined in (4.4.7) *and* (4.4.14). *The matrices satisfy*

$$\mathbf{M}_{j,0}^T \tilde{\mathbf{M}}_{j,0} = \tilde{\mathbf{M}}_{j,0}^T \mathbf{M}_{j,0} = \mathbf{I}. \tag{4.4.17}$$

Furthermore, $S(\Phi_j)$ and $S(\tilde{\Phi}_j)$ are exact of order $d = 4$ and $\tilde{d} = 2$, respectively.

Proof. Equation (4.4.17) follows from the biorthogonality (4.3.34). The remaining assertions have been confirmed above. ■

Proposition 4.6. *Φ_j and $\tilde{\Phi}_j$ are uniformly stable,*

$$\|\varphi_{j,k}\|_{L_2([0,1])}, \qquad \|\tilde{\varphi}_{j,k}\|_{L_2([0,1])} \lesssim 1, \qquad k \in \Delta_j, \quad j \geq j_0. \tag{4.4.18}$$

Furthermore, they are locally finite, i.e., setting

$$\sigma_{j,k} := \operatorname{supp} \varphi_{j,k}, \qquad \tilde{\sigma}_{j,k} := \operatorname{supp} \tilde{\varphi}_{j,k}, \qquad k \in \Delta_j,$$

one has

(4.4.19)

$$\#\{k' \in \Delta_j \colon \sigma_{j,k'} \cap \sigma_{j,k} \neq \emptyset\},\ \#\{k' \in \Delta_j \colon \tilde{\sigma}_{j,k'} \cap \tilde{\sigma}_{j,k} \neq \emptyset\} \lesssim 1 \quad \textit{for all } k \in \Delta_j, \quad j \geq j_0.$$

Proof. This follows as in the proof of Corollary 3.5 in [DKU1]. ■

5. Biorthogonal Multiwavelets on [0, 1]

Given two collections Φ_j, $\tilde{\Phi}_j$ of biorthogonal multigenerators, our goal is now to determine the corresponding collections Ψ_j, $\tilde{\Psi}_j$ of biorthogonal multiwavelets. Following [CDP], this will be accomplished in two steps. First, we identify in Section 5.1 some *initial* complement of $S(\Phi_j)$ in $S(\Phi_{j+1})$ similar to the construction of *hierarchical bases* in a finite element context (see, e.g., [Y]). Then in Section 5.2 we project this complement into the desired complement while preserving stability and compact support of the basis functions.

5.1. *An Initial Stable Completion*

Denoting by $[X, Y]$ the space of bounded linear operators from a normed linear space X into the normed linear space Y, we have for $\mathbf{M}_{j,0}$ from (4.4.7)

$$\mathbf{M}_{j,0} \in [\ell_2(\Delta_j), \ell_2(\Delta_{j+1})], \qquad \|\mathbf{M}_{j,0}\| = \mathcal{O}(1), \qquad j \geq j_0, \tag{5.1.1}$$

see [CDP], where

$$\|\mathbf{M}_{j,0}\| := \sup_{\mathbf{u}\in\ell_2(\Delta_j), \|\mathbf{u}\|_{\ell_2(\Delta_j)}=1} \|\mathbf{M}_{j,0}\mathbf{u}\|_{\ell_2(\Delta_{j+1})}.$$

Define $\nabla_j := \Delta_{j+1} \backslash \Delta_j$. Given $\mathbf{M}_{j,0}$ from (4.4.7), we seek some $\check{\mathbf{M}}_{j,1} \in [\ell_2(\nabla_j), \ell_2(\Delta_{j+1})]$ such that $\check{\mathbf{M}}_j = (\mathbf{M}_{j,0}, \check{\mathbf{M}}_{j,1}) \in [\ell_2(\Delta_j \cup \nabla_j), \ell_2(\Delta_{j+1})]$ is invertible and satisfies

$$\|\check{\mathbf{M}}_j\|, \|\check{\mathbf{M}}_j^{-1}\| = \mathcal{O}(1), \qquad j \geq j_0. \tag{5.1.2}$$

We call $\check{\mathbf{M}}_{j,1}$ an *initial stable completion* of $\mathbf{M}_{j,0}$ since it is usually not yet associated with an appropriate wavelet basis. It is based on the observation that when the generators are *interpolatory*, a basis for a complement of $S(\Phi_j)$ in $S(\Phi_{j+1})$ consists of the functions which interpolate at the grid points contained in Δ_{j+1} but not in Δ_j, i.e., it roughly consists of every second function from Φ_{j+1}.

To construct $\check{\mathbf{M}}_{j,1}$, note that

$$\nabla_j = \Delta_{j+1} \backslash \Delta_j = \{2^j, \ldots, 2^{j+1} - 1\} \tag{5.1.3}$$

so that the cardinality of ∇_j equals $\#\Delta_{j+1} - \#\Delta_j = 2^j$. Let

$$\check{\psi}_{j,k} := \varphi_{j+1,2k+1-2^{j+1}}, \qquad k \in \nabla_j, \tag{5.1.4}$$

see Figure 4 for the indices.

The set $\check{\Psi}_j := \{\check{\psi}_{j,k}, k \in \nabla_j\}$ satisfies

$$(\check{\Psi}_j)^T = \Phi_{j+1}^T \check{\mathbf{M}}_{j,1} \tag{5.1.5}$$

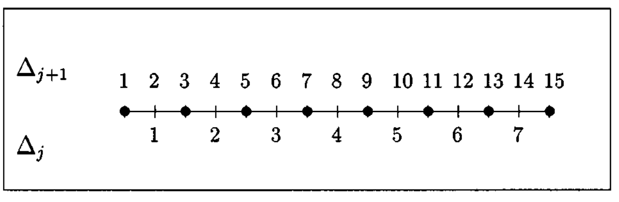

Fig. 4. Index sets Δ_{j+1} and Δ_j for $j = j_0 = 3$; the indices with bullets correspond to the right-hand side of (5.1.4) and represent ∇_j.

with

(5.1.6)
$$\check{\mathbf{M}}_{j,1} := \begin{bmatrix} \mathbf{I} & \mathbf{0} & & & & \\ & \mathbf{0} & & & & \\ & \mathbf{I} & \mathbf{0} & & & \\ & & \mathbf{0} & & & \\ & & \mathbf{I} & & & \\ & & & \ddots & & \\ & & & & \mathbf{I} & \mathbf{0} \\ & & & & & \mathbf{0} \\ & & & & & \mathbf{I} \end{bmatrix} \in \mathbb{R}^{\Delta_{j+1}\times\nabla_j}$$

where $\mathbf{I}, \mathbf{0} \in \mathbb{R}^{2\times 2}$.

In order to confirm that $\check{\mathbf{M}}_{j,1}$ defined in (5.1.6) is indeed an initial stable completion, we need to check (5.1.2), i.e., determine whether

(5.1.7)
$$\check{\mathbf{M}}_j = (\mathbf{M}_{j,0}, \check{\mathbf{M}}_{j,1})$$

have uniformly bounded inverses. Note that the existence of $\check{\mathbf{M}}_j^{-1} = \check{\mathbf{G}}_j = \begin{pmatrix} \check{\mathbf{G}}_{j,0} \\ \check{\mathbf{G}}_{j,1} \end{pmatrix}$ is, in view of (4.4.16) and (5.1.5), equivalent to the *reconstruction formula*

(5.1.8)
$$\Phi_{j+1}^T = \Phi_j^T \check{\mathbf{G}}_{j,0} + \check{\Psi}_j^T \check{\mathbf{G}}_{j,1}.$$

We will use the properties of the specific basis (5.1.4) to see that $\check{\mathbf{G}}_j$ indeed exists, consists also of banded matrices $\check{\mathbf{G}}_{j,0}$, $\check{\mathbf{G}}_{j,1}$, and satisfies $\|\check{\mathbf{G}}_j\| = \mathcal{O}(1)$ independently of j.

To establish the relation (5.1.8), let us for the moment disregard the boundary blocks of $\mathbf{M}_{j,0}$ since they are of fixed size independent of j. In the interior of the interval, the $\varphi_{j,k}$ satisfy the two-scale relation as on all of $\mathbb{R}$,

(5.1.9)
$$\varphi_{j,k} = \frac{1}{\sqrt{2}}(\mathbf{A}_{-1}\varphi_{j+1,2k-1} + \mathbf{A}_0\varphi_{j+1,2k} + \mathbf{A}_1\varphi_{j+1,2k+1}),$$

see (3.2.10). Using the identity for the complement functions (5.1.4) yields

$$\varphi_{j,k} = \frac{1}{\sqrt{2}}(\mathbf{A}_{-1}\check{\psi}_{j,k-1+2^j} + \mathbf{A}_0\varphi_{j+1,2k} + \mathbf{A}_1\check{\psi}_{j,k+2^j})$$

and upon eliminating $\varphi_{j+1,2k}$

(5.1.10)
$$\varphi_{j+1,2k} = \mathbf{A}_0^{-1}(\sqrt{2}\varphi_{j,k} - (\mathbf{A}_{-1}\check{\psi}_{j,k-1+2^j} + \mathbf{A}_1\check{\psi}_{j,k+2^j})),$$

which is as well as (5.1.5) of the form (5.1.8). Recall also from (5.1.4) that $\varphi_{j+1,2k+1} = \check{\psi}_{j,k+2^j}$. With this, we conclude that at least the interior parts of $\check{\mathbf{G}}_{j,0}$, $\check{\mathbf{G}}_{j,1}$ must have the form

(5.1.11)
$$(\check{\mathbf{G}}_{j,0})^I := \sqrt{2}\begin{bmatrix} \mathbf{0} & \mathbf{A}_0^{-1} & \mathbf{0} & & & & & \\ & \mathbf{0} & \mathbf{0} & \mathbf{A}_0^{-1} & & & & \\ & & & \mathbf{0} & \mathbf{0} & \mathbf{A}_0^{-1} & & \\ & & & & & & \ddots & \\ & & & & & & & \mathbf{A}_0^{-1} \\ & & & & & & & & \mathbf{0} \end{bmatrix}$$

and

$$(5.1.12)\quad (\check{\mathbf{G}}_{j,1})^I := \begin{bmatrix} \mathbf{I} & -(\mathbf{A}_0^{-1}\mathbf{A}_{-1})^T & & & & \\ & -(\mathbf{A}_0^{-1}\mathbf{A}_1)^T & \mathbf{I} & -(\mathbf{A}_0^{-1}\mathbf{A}_{-1})^T & & \\ & & & -(\mathbf{A}_0^{-1}\mathbf{A}_1)^T & \mathbf{I} & \\ & & & & \ddots & \\ & & & & & -(\mathbf{A}_0^{-1}\mathbf{A}_{-1})^T \\ & & & & & -(\mathbf{A}_0^{-1}\mathbf{A}_1)^T \quad \mathbf{I} \end{bmatrix}.$$

These matrices clearly have band width independent of j.

In order now to take the boundary effects into account, define $\check{\mathbf{G}}_j = \begin{pmatrix} \check{\mathbf{G}}_{j,0} \\ \check{\mathbf{G}}_{j,1} \end{pmatrix}$ of size $\#\Delta_{j+1}$ as in (5.1.11), (5.1.12) by continuing their block pattern. Then

$$(5.1.13)\qquad \check{\mathbf{M}}_j \check{\mathbf{G}}_j = \begin{bmatrix} \mathbf{N}_L & & \\ & \mathbf{I} & \\ & & \mathbf{N}_R \end{bmatrix} =: \mathbf{N}_j,$$

and the size of $\mathbf{N}_L$, $\mathbf{N}_R$, 10×10, is independent of j. Now we can calculate

$$\mathbf{N}_L = \begin{bmatrix} 1 & & 0.5 & 0.25 & & & & & & \\ & 1 & -0.75 & 1.25 & & & & & & \\ & & 0.5 & 0.25 & & & 0.5 & -0.25 & & \\ & & -0.75 & -0.25 & & & 0.75 & -0.25 & & \\ & & 0.5 & 0.5 & 1 & & -0.5 & 2.5 & & \\ & & 3 & 2 & & 1 & -3 & 4 & & \\ & & 5 & 4 & & & -4 & 8 & & \\ & & 6 & 5 & & & -6 & 8 & & \\ & & 4 & 3.25 & & & -4 & 5.75 & 1 & \\ & & -5.25 & -4.25 & & & 5.25 & -7.75 & & 1 \end{bmatrix}$$

and similarly $\mathbf{N}_R$. We can check that $\mathbf{N}_L$ and $\mathbf{N}_R$ are nonsingular. For $j = j_0 = 3$, we display the nonzero pattern of $\mathbf{N}_3$ and its inverse in Figure 5.

Setting

$$(5.1.14)\qquad \check{\mathbf{G}}_j^{\text{new}} := \check{\mathbf{G}}_j \mathbf{N}_j^{-1}$$

yields

$$\check{\mathbf{M}}_j \check{\mathbf{G}}_j^{\text{new}} = \mathbf{I}$$

by (5.1.13). Thus, we have proved the following result:

Proposition 5.1. *The matrix* $\check{\mathbf{M}}_{j,1}$ *defined in* (5.1.6) *is a stable completion of* $\mathbf{M}_{j,0}$, *i.e.,* $\check{\mathbf{M}}_j = (\mathbf{M}_{j,0}, \check{\mathbf{M}}_{j,1})$ *is invertible and satisfies* (5.1.2).

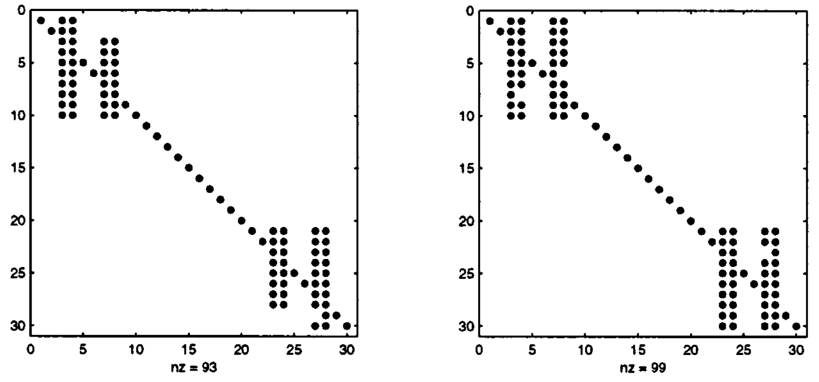

Fig. 5. Nonzero pattern of transformation matrix $\mathbf{N}_3$ and its inverse $\mathbf{N}_3^{-1}$.

5.2. *Biorthogonal Multiwavelets on* [0, 1]

We can now apply Corollary 3.1 from [CDP] to obtain

Corollary 5.2. *The matrix*

$$\mathbf{M}_{j,1} := (\mathbf{I} - \mathbf{M}_{j,0}\tilde{\mathbf{M}}_{j,0}^T)\check{\mathbf{M}}_{j,1} \tag{5.2.1}$$

is also a stable completion of $\mathbf{M}_{j,0}$, *i.e.*,

$$\mathbf{M}_j := (\mathbf{M}_{j,0}, \mathbf{M}_{j,1})$$

has a uniformly bounded inverse, and $\mathbf{G}_j := \mathbf{M}_j^{-1}$ *has the form*

$$\mathbf{G}_j = \begin{pmatrix} \tilde{\mathbf{M}}_{j,0}^T \\ \check{\mathbf{G}}_{j,1}^{\text{new}} \end{pmatrix}. \tag{5.2.2}$$

Moreover, the collections of primal and dual multiwavelets

$$\Psi_j := \mathbf{M}_{j,1}^T \Phi_{j+1}, \qquad \tilde{\Psi}_j := \check{\mathbf{G}}_{j,1}^{\text{new}} \tilde{\Phi}_{j+1}, \tag{5.2.3}$$

form biorthogonal systems,

$$(\Psi_j, \tilde{\Psi}_j)_{[0,1]} = \mathbf{I}, \qquad (\Psi_j, \tilde{\Phi}_j)_{[0,1]} = (\Phi_j, \tilde{\Psi}_j)_{[0,1]} = \mathbf{0}. \tag{5.2.4}$$

Relation (5.2.4) implies that the collections

$$\Psi = \Phi_{j_0} \cup \bigcup_{j \geq j_0} \Psi_j, \qquad \tilde{\Psi} := \tilde{\Phi}_{j_0} \cup \bigcup_{j \geq j_0} \tilde{\Psi}_j,$$

are biorthogonal,

$$(\Psi_j, \tilde{\Psi}_{j'})_{[0,1]} = \delta_{j,j'}\mathbf{I}, \qquad j, j' \geq j_0 - 1, \tag{5.2.5}$$

where we have set $\psi_{j_0-1,k} := \varphi_{j_0,k}$ and $\tilde{\psi}_{j_0-1,k} := \tilde{\varphi}_{j_0,k}$ with $\nabla_{j_0-1} := \Delta_{j_0}$.

Defining

$$\mathbf{L}_j = -\tilde{\mathbf{M}}_{j,0}^T \check{\mathbf{M}}_{j,1}, \tag{5.2.6}$$

it can be seen that the new complement functions $\psi_{j,k}$ are obtained by updating the initial complement functions $\check{\psi}_{j,k}$ by a linear combination of the coarse generators $\varphi_{j,k}$. In fact, by (5.2.1) and (4.4.16),

$$\Psi_j^T = \Phi_{j+1}^T \mathbf{M}_{j,1} = \Phi_{j+1}^T \check{\mathbf{M}}_{j,1} + \Phi_{j+1}^T \mathbf{M}_{j,0} \mathbf{L}_j = \check{\Psi}_j^T + \Phi_j^T \mathbf{L}_j,$$

i.e.,

$$\psi_{j,k} = \check{\psi}_{j,k} + \sum_{l \in \Delta_j} (\mathbf{L}_j)_{l,k} \varphi_{j,l}, \qquad k \in \nabla_j. \tag{5.2.7}$$

Thus, by construction, the Ψ_j naturally have local support in the sense that

$$\operatorname{diam}(\operatorname{supp} \psi_{j,k}) \sim \operatorname{diam}(\operatorname{supp} \tilde{\psi}_{j,k}) \sim 2^{-j}, \qquad k \in \nabla_j,$$

since $\mathbf{L}_j$ is banded.

The nonzero pattern of the refinement matrices $\mathbf{M}_{3,0}$, $\tilde{\mathbf{M}}_{3,0}$ and its completions $\mathbf{M}_{3,1}$, $\check{\mathbf{G}}_{3,1}^T$ is depicted in Figures 6 and 7, respectively. The exact data can be found in the Appendix.

Of course, for any other level $j > 3$, $\mathbf{M}_j$ and $\mathbf{G}_j$ can immediately be assembled by simply extending the stationary interior part accordingly while retaining the boundary blocks.

Note that the correctness of the mask coefficients of the biorthogonal wavelets Ψ_j, $\tilde{\Psi}_j$ can be confirmed by checking $\mathbf{M}_j \mathbf{G}_j = \mathbf{I}$.

5.3. *Jackson and Bernstein Estimates, Norm Equivalences*

Since Φ_j, $\tilde{\Phi}_j$ are biorthogonal (4.3.34) and exact of order 4 and 2, respectively, Propositions 4.5 and 4.6, combined with [DKU1, Lemma 2.1], yield

Corollary 5.3. *One has*

$$\inf_{v_j \in V_j} \|v - v_j\|_{L_2([0,1])} \lesssim 2^{-sj} \|v\|_{H^s([0,1])}, \qquad v \in H^s([0,1]), \tag{5.3.1}$$

where

$$s \leq \begin{cases} d = 4, & V_j = S(\Phi_j), \\ \tilde{d} = 2, & V_j = S(\tilde{\Phi}_j). \end{cases} \tag{5.3.2}$$

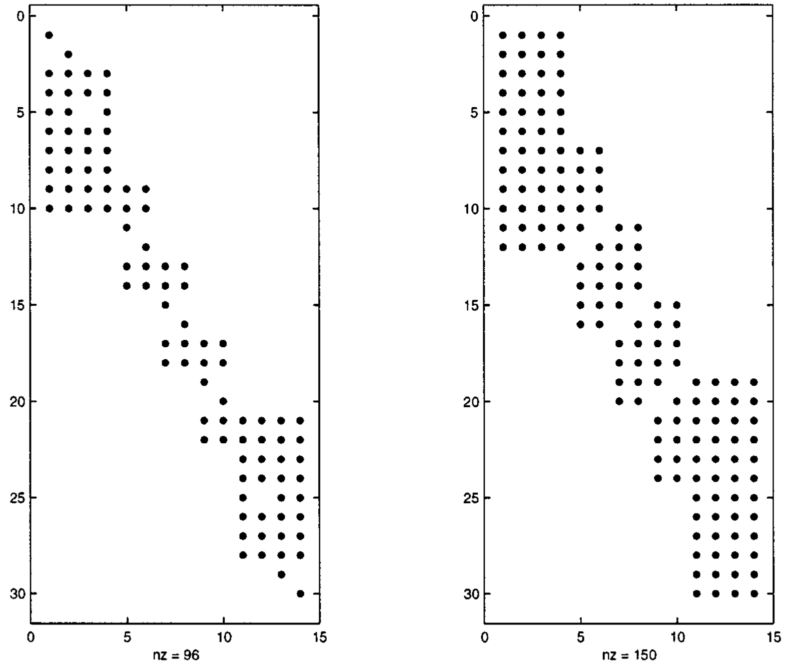

Fig. 6. Nonzero pattern of refinement matrices $\mathbf{M}_{3,0}$, $\tilde{\mathbf{M}}_{3,0}$.

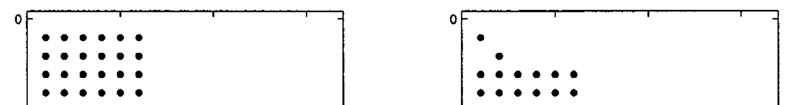

Fig. 7. Nonzero pattern of completion matrices $\mathbf{M}_{3,1}$, $(\check{\mathbf{G}}_{3,1}^{\mathrm{new}})^T$.

Using the fact that φ consists of $\mathcal{C}^1$ piecewise cubic polynomials, one can show that

$$\gamma := \sup\{s : \varphi \in H^s(\mathbb{R})\} = \tfrac{5}{2}. \tag{5.3.3}$$

Recalling that $\tilde{\gamma} = 0.824926$ (3.1.3), the following fact follows from [D3].

Corollary 5.4. *The inverse estimate*

$$\|v_j\|_{H^s([0,1])} \lesssim 2^{sj} \|v_j\|_{L_2([0,1])}, \qquad v_j \in V_j, \tag{5.3.4}$$

holds where

$$s < \begin{cases} \gamma = \frac{5}{2}, & V_j = S(\Phi_j), \\ \tilde{\gamma} = 0.824926, & V_j = S(\tilde{\Phi}_j). \end{cases} \tag{5.3.5}$$

Combining Corollaries 5.3 and 5.4 with [D2, Theorem 4.2], provides the following main result:

Theorem 5.5. *One has for any $v \in H^s([0,1])$ the norm equivalences*

$$\begin{aligned} &\|(v, \tilde{\Phi}_{j_0})_{[0,1]}\|^2_{\ell_2(\Delta_{j_0})} + \sum_{j=j_0}^{\infty} 2^{2sj} \|(v, \tilde{\Psi}_j)_{[0,1]}\|^2_{\ell_2(\nabla_j)} \\ &\qquad \sim \begin{cases} \|v\|^2_{H^s([0,1])}, & s \in [0, \frac{5}{2}), \\ \|v\|^2_{(H^{-s}([0,1]))^*}, & s \in (-0.824926, 0). \end{cases} \end{aligned} \tag{5.3.6}$$

Here for $s < 0$, $H^s([0,1])$ means the dual $(H^{-s}([0,1]))^*$ of $H^{-s}([0,1])$, relative to $(\cdot,\cdot)_{L_2([0,1])}$.

In particular, the primal and dual multiwavelets form Riesz bases for $L_2([0,1])$.

6. Visualization of the Functions

Finally, we visualize the functions $\Phi_j, \tilde{\Phi}_j, \Psi_j, \tilde{\Psi}_j$ for $j = j_0 = 3$. Note that the two functions in $\psi_{3,8}$, or the two components in $\psi_{3,15}$, respectively, look very similar. Therefore, we have added Figure 12 to clarify the distinction of these functions. (The functions have been normalized to satisfy $(\psi_1)_{3,8}(0) = (\psi_2)_{3,8}(0)$ and $(\psi_1)_{3,15}(1) = (\psi_1)_{3,15}(1)$.)

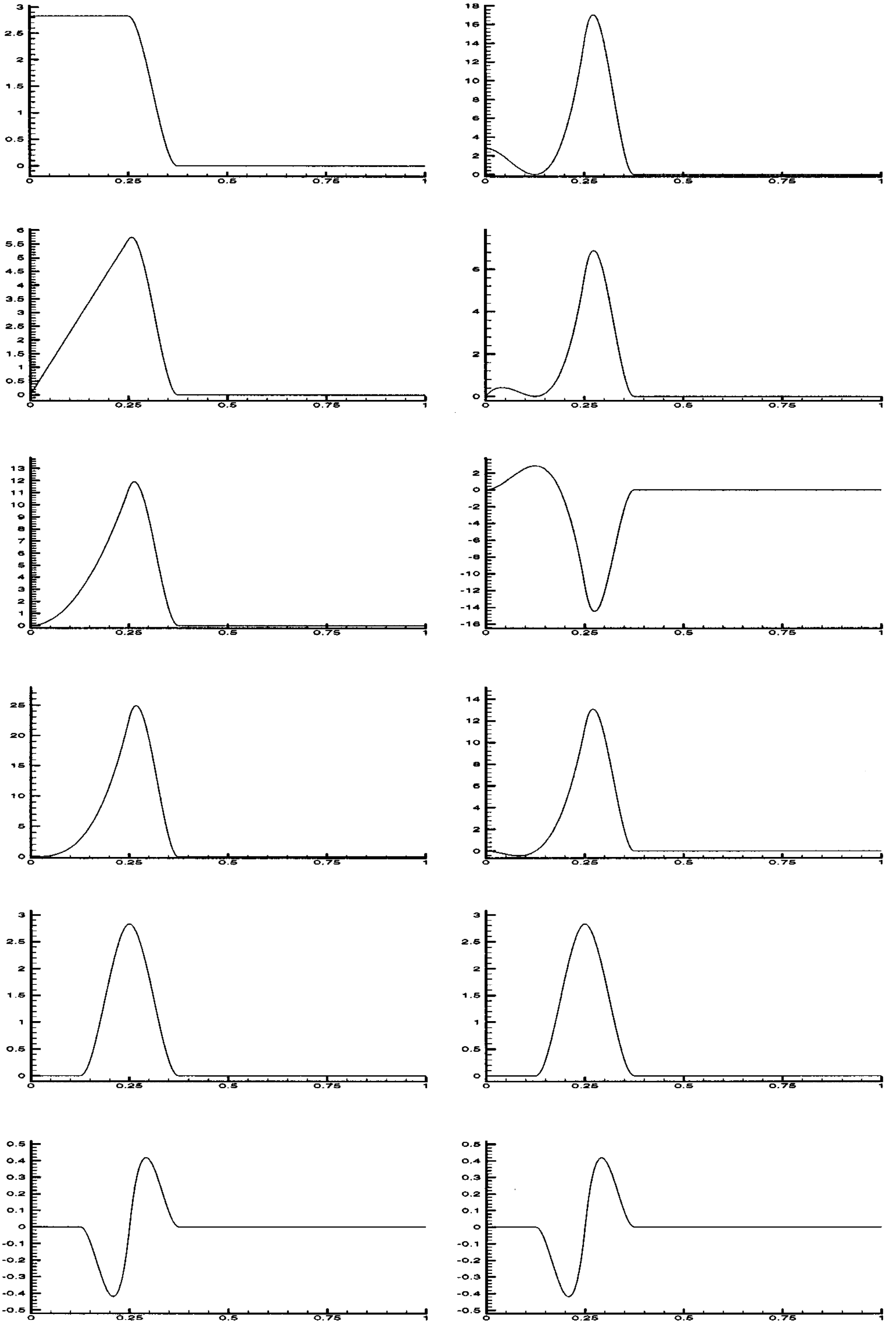

Fig. 8. Primal multigenerators $\varphi_{3,k}$ before (left column) and after (right column) biorthogonalization (in the order of Φ_j), at the left boundary; we here dispense with the boundary adapted ones at the right boundary since they are symmetric to the ones at the left boundary.

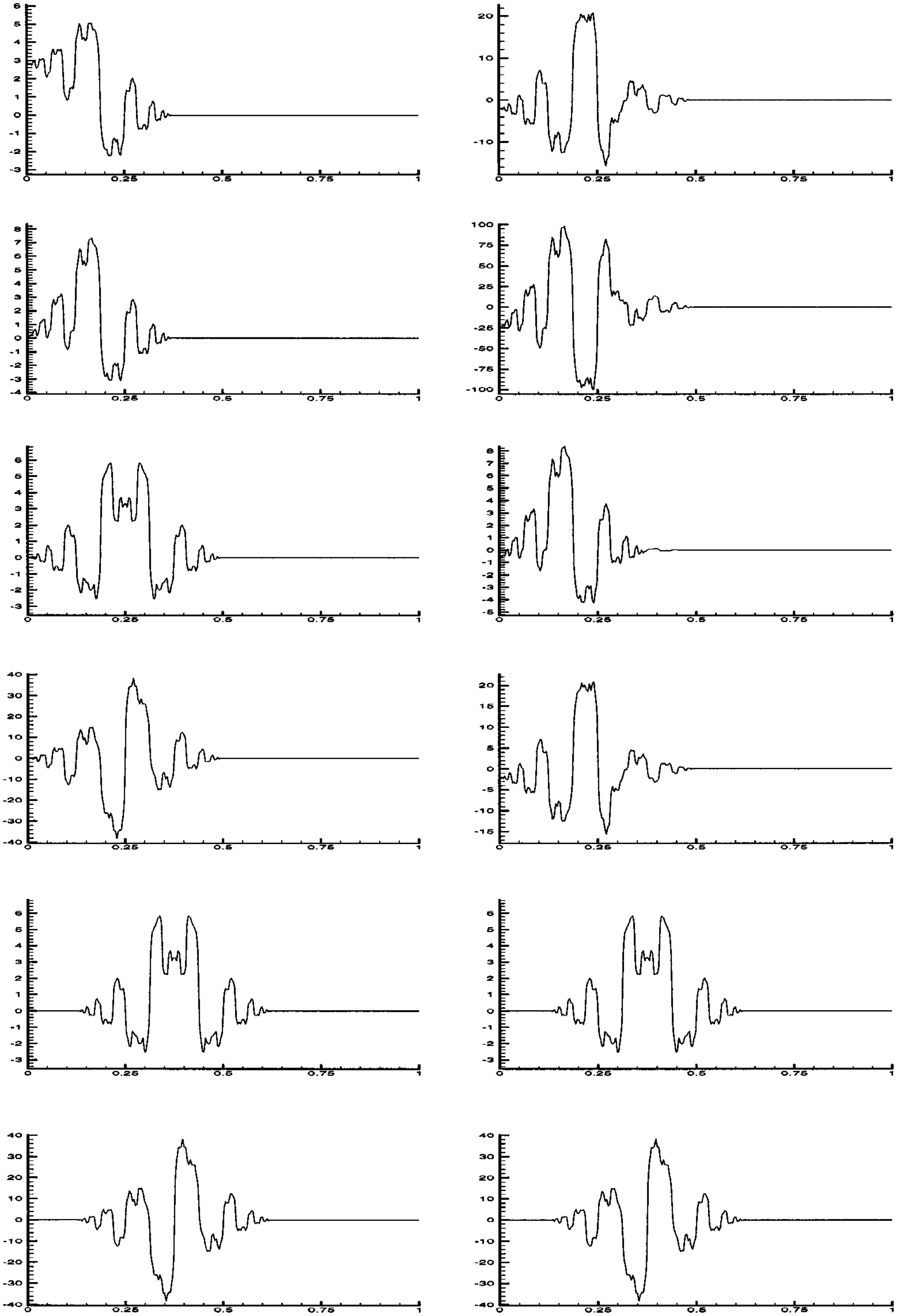

Fig. 9. Dual multigenerators $\tilde{\varphi}_{3,k}$ and after (right column) biorthogonalization (in the order of $\tilde{\Phi}_j$), at the left boundary; we dispense here with the boundary adapted ones at the right boundary since they are symmetric to the ones at the left boundary.

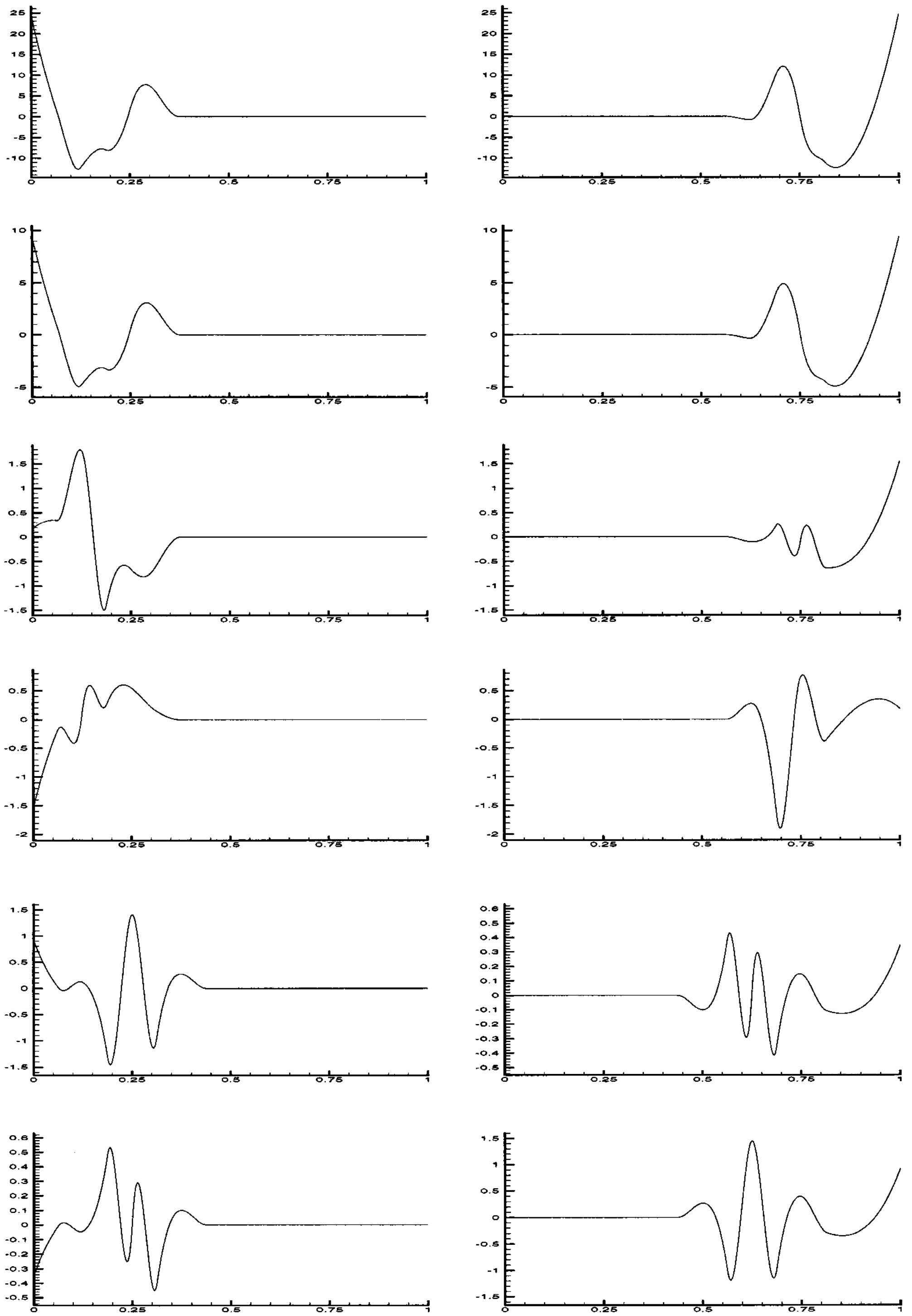

Fig. 10. Primal multiwavelets $\psi_{3,8}, \ldots, \psi_{3,10}$ (left column) and $\psi^{\updownarrow}_{3,15}, \ldots, \psi^{\updownarrow}_{3,13}$ (right column).

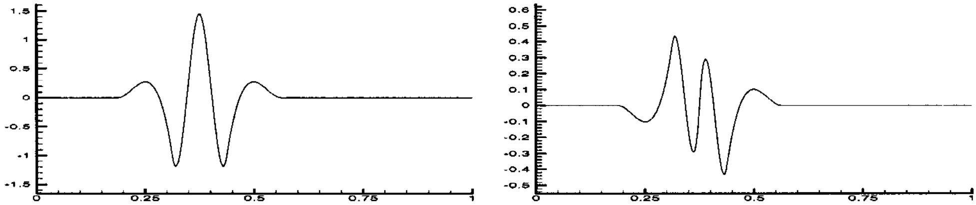

Fig. 11. Primal multiwavelets $\psi_{3,11}$ as an example for the interior ones; first component (left), second component (right).

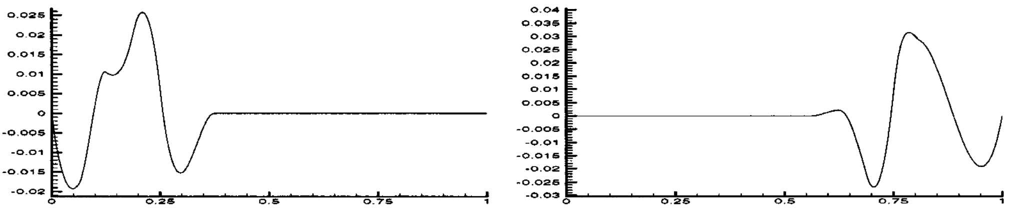

Fig. 12. Difference between the (scaled) primal multiwavelets $(\psi_1)_{3,8}$ and $(\psi_2)_{3,8}$ (left) and $(\psi_1)_{3,15}$ and $(\psi_2)_{3,15}$ (right).

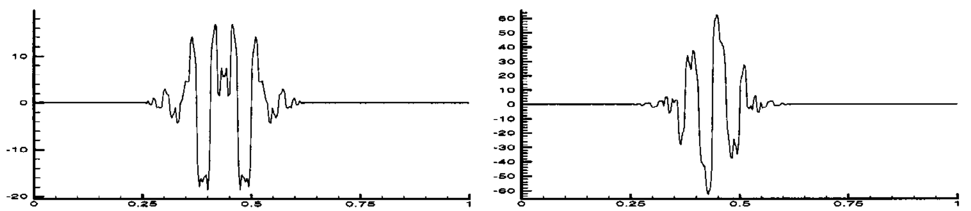

Fig. 13. Dual multiwavelets $\tilde{\varphi}_{3,11}$ as an example for the interior ones; first component (left), second component (right).

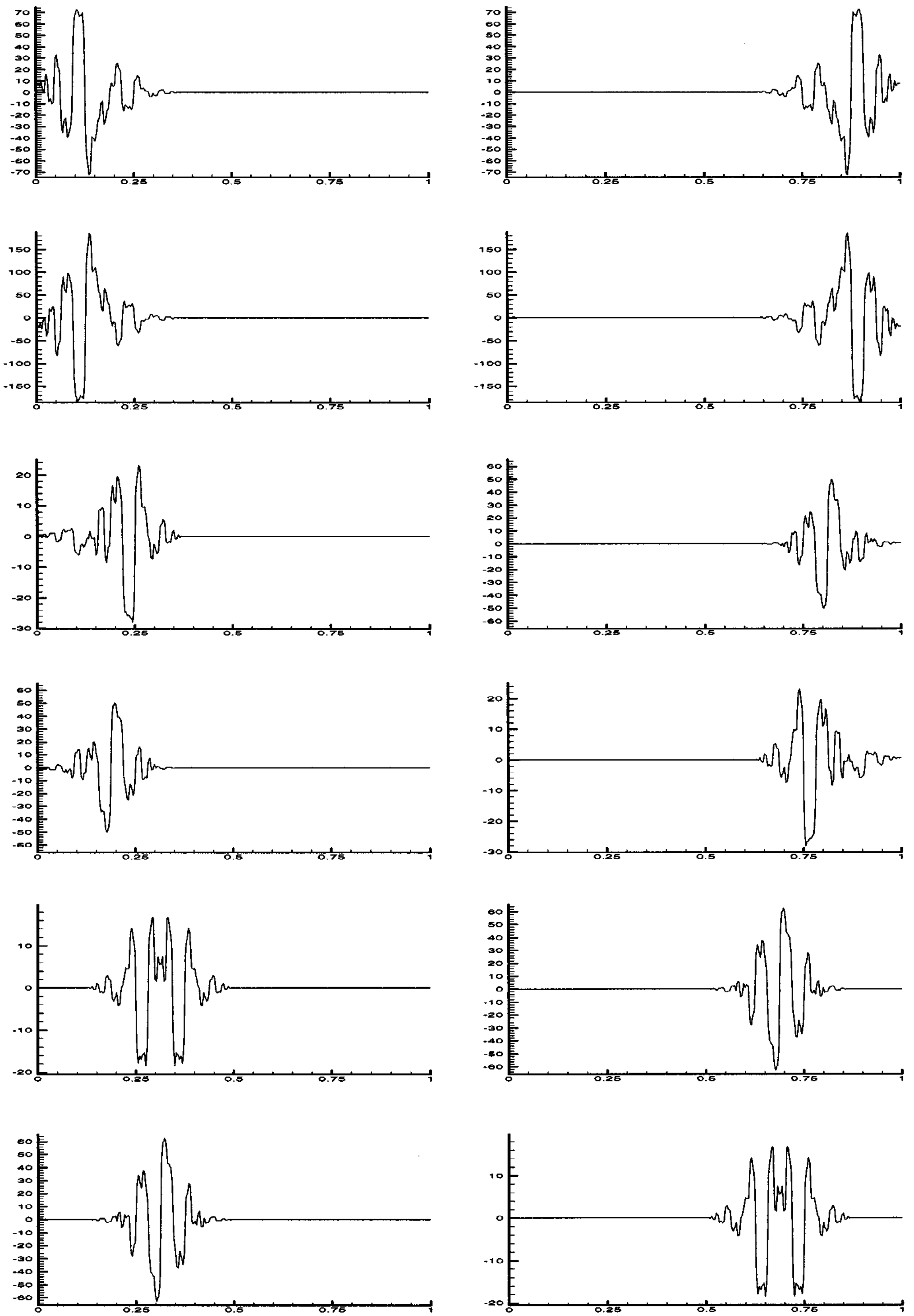

Fig. 14. Dual multiwavelets $\tilde{\varphi}_{3,8}, \ldots, \tilde{\varphi}_{3,10}$ (left column) and $\tilde{\varphi}^{\updownarrow}_{3,15}, \ldots, \tilde{\varphi}^{\updownarrow}_{3,13}$ (right column).

7. Appendix

We display here the positions and the nonzero entries of the matrices $\mathbf{M}_3$ and $\mathbf{G}_3$.

$\mathbf{M}_3 =$

(1, 1)	7.071067811865475e−01	(3, 1)	3.535533905932734e−01	(4, 1)	−5.303300858899110e−01
(5, 1)	7.071067811865488e−01	(6, 1)	1.590990257669735e+00	(7, 1)	3.535533905932743e+00
(8, 1)	4.242640687119291e+00	(9, 1)	2.828427124746195e+00	(10, 1)	−3.712310601229381e+00
(2, 2)	3.535533905932737e−01	(3, 2)	8.838834764831818e−02	(4, 2)	−8.838834764831871e−02
(5, 2)	2.651650429449557e−01	(6, 2)	6.187184335382316e−01	(7, 2)	1.414213562373100e+00
(8, 2)	1.767766952966375e+00	(9, 2)	1.149048519428143e+00	(10, 2)	−1.502601910021419e+00
(3, 3)	3.535533905932741e−01	(4, 3)	5.303300858899110e−01	(6, 3)	−1.590990257669735e+00
(7, 3)	−2.828427124746195e+00	(8, 3)	−4.242640687119291e+00	(9, 3)	−2.474873734152921e+00
(10, 3)	3.181980515339470e+00	(3, 4)	−8.838834764831850e−02	(4, 4)	−8.838834764831854e−02
(5, 4)	7.954951288348655e−01	(6, 4)	1.325825214724777e+00	(7, 4)	2.828427124746191e+00
(8, 4)	2.828427124746191e+00	(9, 4)	2.121320343559643e+00	(10, 4)	−2.828427124746191e+00
(9, 5)	3.535533905932737e−01	(10, 5)	5.303300858899106e−01	(11, 5)	7.071067811865475e−01
(13, 5)	3.535533905932737e−01	(14, 5)	−5.303300858899106e−01	(9, 6)	−8.838834764831843e−02
(10, 6)	−8.838834764831843e−02	(12, 6)	3.535533905932737e−01	(13, 6)	8.838834764831843e−02
(14, 6)	−8.838834764831843e−02	(13, 7)	3.535533905932737e−01	(14, 7)	5.303300858899106e−01
(15, 7)	7.071067811865475e−01	(17, 7)	3.535533905932737e−01	(18, 7)	−5.303300858899106e−01
(13, 8)	−8.838834764831843e−02	(14, 8)	−8.838834764831843e−02	(16, 8)	3.535533905932737e−01
(17, 8)	8.838834764831843e−02	(18, 8)	−8.838834764831843e−02	(17, 9)	3.535533905932737e−01
(18, 9)	5.303300858899106e−01	(19, 9)	7.071067811865475e−01	(21, 9)	3.535533905932737e−01
(22, 9)	−5.303300858899106e−01	(17, 10)	−8.838834764831843e−02	(18, 10)	−8.838834764831843e−02
(20, 10)	3.535533905932737e−01	(21, 10)	8.838834764831843e−02	(22, 10)	−8.838834764831843e−02
(21, 11)	2.121320343559643e+00	(22, 11)	2.828427124746191e+00	(23, 11)	2.828427124746191e+00
(24, 11)	−2.828427124746191e+00	(25, 11)	7.954951288348655e−01	(26, 11)	−1.325825214724777e+00
(27, 11)	−8.838834764831877e−02	(28, 11)	−8.838834764831850e−02	(21, 12)	−2.474873734152921e+00
(22, 12)	−3.181980515339470e+00	(23, 12)	−2.828427124746195e+00	(24, 12)	4.242640687119291e+00
(26, 12)	1.590990257669735e+00	(27, 12)	5.303300858899116e−01	(28, 12)	3.535533905932741e−01
(21, 13)	1.149048519428143e+00	(22, 13)	1.502601910021419e+00	(23, 13)	1.414213562373100e+00
(24, 13)	−1.767766952966375e+00	(25, 13)	2.651650429449559e−01	(26, 13)	−6.187184335382316e−01
(27, 13)	−8.838834764831932e−02	(28, 13)	8.838834764831816e−02	(29, 13)	3.535533905932737e−01
(21, 14)	2.828427124746195e+00	(22, 14)	3.712310601229381e+00	(23, 14)	3.535533905932743e+00
(24, 14)	−4.242640687119291e+00	(25, 14)	7.071067811865483e−01	(26, 14)	−1.590990257669735e+00
(27, 14)	−5.303300858899119e−01	(28, 14)	3.535533905932732e−01	(30, 14)	7.071067811865475e−01
(1, 15)	8.697265624999993e+00	(2, 15)	−1.906787109374998e+01	(3, 15)	−3.683380126953116e+00
(4, 15)	−4.811737060546865e+00	(5, 15)	−4.510192871093750e−01	(6, 15)	3.570831298828038e+00
(7, 15)	7.421874999998295e−01	(8, 15)	−2.302734375000217e+00	(9, 15)	−2.045898437500888e−01
(10, 15)	1.904296875016342e−02	(1, 16)	3.348307291666665e+00	(2, 16)	−6.979492187499997e+00
(3, 16)	−1.438476562499997e+00	(4, 16)	−2.056762695312496e+00	(5, 16)	−1.841634114583353e−01
(6, 16)	1.460327148437460e+00	(7, 16)	3.046874999999218e−01	(8, 16)	−9.453125000001013e−01
(9, 16)	−8.398437500004530e−02	(10, 16)	7.812500000078160e−03	(1, 17)	6.250000000000035e−02
(2, 17)	2.988281249999999e−01	(3, 17)	3.674316406249976e−02	(4, 17)	−2.735595703125007e−01
(5, 17)	4.197998046875016e−01	(6, 17)	−3.625488281249556e−02	(7, 17)	−2.499999999999916e−01
(8, 17)	7.734375000000107e−01	(9, 17)	6.835937500000711e−02	(10, 17)	−5.859375000009326e−03
(1, 18)	−5.494791666666665e−01	(2, 18)	1.251953125000000e+00	(3, 18)	1.717529296874995e−01
(4, 18)	2.725830078124994e−01	(5, 18)	−9.281412760416624e−02	(6, 18)	7.911376953125066e−01
(7, 18)	−9.374999999998757e−02	(8, 18)	2.890625000000164e−01	(9, 18)	2.539062500000777e−02
(10, 18)	−1.953125000012879e−03	(1, 19)	3.281249999999999e−01	(2, 19)	−8.847656249999999e−01
(3, 19)	−1.148681640624996e−01	(4, 19)	−8.679199218749953e−02	(5, 19)	1.094970703124994e−01
(6, 19)	−3.112792968750511e−02	(7, 19)	−2.500000000000104e−01	(8, 19)	−7.734375000000122e−01
(9, 19)	3.632812499999938e−01	(11, 19)	−2.499999999999999e−01	(12, 19)	7.734374999999999e−01
(13, 19)	6.835937500000000e−02	(14, 19)	−5.859375000000000e−03	(1, 20)	−1.223958333333333e−01
(2, 20)	3.300781249999999e−01	(3, 20)	4.284667968749986e−02	(4, 20)	3.234863281249982e−02
(5, 20)	−4.073079427083309e−02	(6, 20)	1.184082031250189e−02	(7, 20)	9.375000000000389e−02
(8, 20)	2.890625000000048e−01	(10, 20)	7.148437499999960e−01	(11, 20)	−9.374999999999999e−02
(12, 20)	2.890624999999999e−01	(13, 20)	2.539062499999999e−02	(14, 20)	−1.953125000000000e−03
(9, 21)	6.835937500000000e−02	(10, 21)	5.859375000000000e−03	(11, 21)	−2.499999999999999e−01
(12, 21)	−7.734374999999999e−01	(13, 21)	3.632812500000001e−01	(15, 21)	−2.499999999999999e−01
(16, 21)	7.734374999999999e−01	(9, 22)	−2.539062499999999e−02	(10, 22)	−1.953125000000000e−03
(11, 22)	9.374999999999999e−02	(12, 22)	2.890624999999999e−01	(14, 22)	7.148437500000000e−01
(15, 22)	−9.374999999999999e−02	(16, 22)	2.890624999999999e−01	(21, 23)	6.835937500000000e−02
(22, 23)	−5.859375000000000e−03	(13, 24)	−2.539062499999999e−02	(14, 24)	−1.953125000000000e−03
(15, 24)	9.374999999999999e−02	(16, 24)	2.890624999999999e−01	(18, 24)	7.148437500000000e−01
(19, 24)	−9.374999999999999e−02	(20, 24)	2.890624999999999e−01	(21, 24)	2.539062499999999e−02
(22, 24)	−1.953125000000000e−03	(17, 25)	6.835937500000000e−02	(18, 25)	5.859375000000000e−03

(19, 25)	−2.499999999999999e−01	(20, 25)	−7.734374999999999e−01	(21, 25)	3.632812499999942e−01
(23, 25)	−2.500000000000104e−01	(24, 25)	7.734375000000122e−01	(25, 25)	1.094970703124986e−01
(26, 25)	3.112792968750511e−02	(27, 25)	−8.679199218749856e−02	(28, 25)	−1.148681640624996e−01
(29, 25)	−8.847656249999999e−01	(30, 25)	3.281249999999999e−01	(17, 26)	−2.539062499999999e−02
(18, 26)	−1.953125000000000e−03	(19, 26)	9.374999999999999e−02	(20, 26)	2.890624999999999e−01
(22, 26)	7.148437499999960e−01	(23, 26)	−9.375000000000400e−02	(24, 26)	2.890625000000046e−01
(25, 26)	4.073079427083280e−02	(26, 26)	1.184082031250189e−02	(27, 26)	−3.234863281249945e−02
(28, 26)	−4.284667968749988e−02	(29, 26)	−3.300781249999999e−01	(30, 26)	1.223958333333333e−01
(21, 27)	6.835937500000627e−02	(22, 27)	5.859375000008771e−03	(23, 27)	−2.499999999999923e−01
(24, 27)	−7.734375000000093e−01	(25, 27)	4.197998046875018e−01	(26, 27)	3.625488281249586e−02
(27, 27)	−2.735595703125012e−01	(28, 27)	3.674316406249978e−02	(29, 27)	2.988281249999999e−01
(30, 27)	6.250000000000035e−02	(21, 28)	−2.539062500000666e−02	(22, 28)	−1.953125000013767e−03
(23, 28)	9.374999999998623e−02	(24, 28)	2.890625000000164e−01	(25, 28)	9.281412760416502e−02
(26, 28)	7.911376953125071e−01	(27, 28)	−2.725830078124982e−01	(28, 28)	−1.717529296874996e−01
(29, 28)	−1.251953125000000e+00	(30, 28)	5.494791666666665e−01	(21, 29)	−8.398437500003730e−02
(22, 29)	−7.812500000081712e−03	(23, 29)	3.046874999999218e−01	(24, 29)	9.453125000000888e−01
(25, 29)	−1.841634114583415e−01	(26, 29)	−1.460327148437461e+00	(27, 29)	−2.056762695312488e+00
(28, 29)	−1.438476562499997e+00	(29, 29)	−6.979492187499996e+00	(30, 29)	3.348307291666665e+00
(21, 30)	−2.045898437500746e−01	(22, 30)	−1.904296875016342e−02	(23, 30)	7.421874999998224e−01
(24, 30)	2.302734375000206e+00	(25, 30)	−4.510192871093919e−01	(26, 30)	−3.570831298828040e+00
(27, 30)	−4.811737060546847e+00	(28, 30)	−3.683380126953118e+00	(29, 30)	−1.906787109374998e+01
(30, 30)	8.697265624999993e+00				

$\mathbf{G}_3 =$

(1, 1)	−1.088557744006321e+01	(2, 1)	5.393208381272626e+01	(3, 1)	5.887147327154208e+00
(4, 1)	−7.734325686210864e+00	(15, 1)	1.000000000000000e+00	(1, 2)	−4.735221582867725e+00
(2, 2)	2.256941214482531e+01	(3, 2)	2.390858768289280e+00	(4, 2)	−3.082543624235105e+00
(16, 2)	1.000000000000000e+00	(1, 3)	1.186613567178674e+01	(2, 3)	−5.086196979987922e+01
(3, 3)	−4.788162520261248e+00	(4, 3)	6.053220745977807e+00	(15, 3)	−5.925925925925930e−01
(16, 3)	−8.888888888888875e−01	(17, 3)	−2.592592592592584e−01	(18, 3)	4.444444444444446e−01
(1, 4)	−8.960368742848280e+00	(2, 4)	4.224410590416819e+01	(3, 4)	4.539570292500354e+00
(4, 4)	−5.569846969776066e+00	(15, 4)	1.777777777777773e+00	(16, 4)	−2.666666666666668e+00
(17, 4)	−2.222222222222180e−01	(18, 4)	3.333333333333372e−01	(1, 5)	−8.838834764831893e−02
(2, 5)	−8.452135743870448e−01	(3, 5)	4.681820289496869e−01	(4, 5)	1.089662598351926e+00
(17, 5)	1.000000000000000e+00	(1, 6)	7.770808897414662e−01	(2, 6)	−3.541058177660757e+00
(3, 6)	−2.260347848714810e−01	(4, 6)	6.062888221501843e−01	(18, 6)	1.000000000000000e+00
(1, 7)	8.838834764831844e−01	(2, 7)	−4.176349426383046e+00	(3, 7)	−1.712524235686170e−01
(4, 7)	1.027514541411702e+00	(5, 7)	−7.733980419227862e−02	(6, 7)	4.806116403377315e−01
(15, 7)	−4.074074074074056e−01	(16, 7)	8.888888888888886e−01	(17, 7)	−7.407407407407409e−01
(18, 7)	−4.444444444444450e−01	(19, 7)	−5.000000000000009e−01	(20, 7)	7.499999999999993e−01
(1, 8)	−6.113527379008691e−01	(2, 8)	2.994155276586786e+00	(3, 8)	1.114061465150680e−01
(4, 8)	−6.214805694022389e−01	(5, 8)	−5.524271728019902e−02	(6, 8)	3.425048471372339e−01
(15, 8)	4.444444444444423e−01	(16, 8)	−9.999999999999998e−01	(17, 8)	4.444444444444454e−01
(19, 8)	−2.499999999999986e−01	(20, 8)	2.500000000000003e−01	(1, 9)	−4.640388251536717e−01
(2, 9)	2.502495092793016e+00	(3, 9)	2.347815484408458e−02	(4, 9)	−5.593325124620151e−01
(5, 9)	3.535533905932737e−01	(6, 9)	−2.187611604295881e+00	(19, 9)	1.000000000000000e+00
(1, 10)	1.730938474779569e−01	(2, 10)	−9.336019220353635e−01	(3, 10)	−8.746763569364843e−03
(4, 10)	2.085412577327513e−01	(5, 10)	1.325825214724776e−01	(6, 10)	−8.175922157469455e−01
(20, 10)	1.000000000000000e+00	(1, 11)	1.021990269683682e−01	(2, 11)	−5.510461048699853e−01
(3, 11)	−5.179004745018657e−03	(4, 11)	1.232603129314441e−01	(5, 11)	8.617863895711048e−01
(7, 11)	−7.733980419227862e−02	(8, 11)	4.806116403377315e−01	(19, 11)	−5.000000000000000e−01
(20, 11)	−7.500000000000000e−01	(21, 11)	−5.000000000000000e−01	(22, 11)	7.500000000000000e−01
(1, 12)	−7.273624441892870e−02	(2, 12)	3.922232926894130e−01	(3, 12)	3.682847818679935e−03
(4, 12)	−8.769781368231594e−02	(6, 12)	1.325825214724776e+00	(7, 12)	−5.524271728019902e−02
(8, 12)	3.425048471372339e−01	(19, 12)	2.500000000000000e−01	(20, 12)	2.500000000000000e−01
(21, 12)	−2.500000000000000e−01	(22, 12)	2.500000000000000e−01	(5, 13)	3.535533905932737e−01
(6, 13)	2.187611604295881e+00	(7, 13)	3.535533905932737e−01	(8, 13)	−2.187611604295881e+00
(21, 13)	1.000000000000000e+00	(5, 14)	−1.325825214724776e−01	(6, 14)	−8.175922157469455e−01
(7, 14)	1.325825214724776e−01	(8, 14)	−8.175922157469455e−01	(22, 14)	1.000000000000000e+00
(5, 15)	−7.733980419227862e−02	(6, 15)	−4.806116403377315e−01	(7, 15)	8.617863895711048e−01
(9, 15)	−7.733980419227862e−02	(10, 15)	4.806116403377315e−01	(21, 15)	−5.000000000000000e−01
(22, 15)	−7.500000000000000e−01	(23, 15)	−5.000000000000000e−01	(24, 15)	7.500000000000000e−01
(5, 16)	5.524271728019902e−02	(6, 16)	3.425048471372339e−01	(8, 16)	1.325825214724776e+00
(9, 16)	−5.524271728019902e−02	(10, 16)	3.425048471372339e−01	(21, 16)	2.500000000000000e−01
(22, 16)	2.500000000000000e−01	(23, 16)	−2.500000000000000e−01	(24, 16)	2.500000000000000e−01
(7, 17)	3.535533905932737e−01	(8, 17)	2.187611604295881e+00	(9, 17)	3.535533905932737e−01
(10, 17)	−2.187611604295881e+00	(23, 17)	1.000000000000000e+00	(7, 18)	−1.325825214724776e−01
(8, 18)	−8.175922157469455e−01	(9, 18)	1.325825214724776e−01	(10, 18)	−8.175922157469455e−01
(24, 18)	1.000000000000000e+00	(7, 19)	−7.733980419227862e−02	(8, 19)	−4.806116403377315e−01

(9, 19)	8.617863895711048e−01	(11, 19)	1.232603129314441e−01	(12, 19)	−5.179004745018657e−03
(13, 19)	−5.510461048699853e−01	(14, 19)	1.021990269683682e−01	(23, 19)	−5.000000000000000e−01
(24, 19)	−7.500000000000000e−01	(25, 19)	−5.000000000000000e−01	(26, 19)	7.500000000000000e−01
(7, 20)	5.524271728019902e−02	(8, 20)	3.425048471372339e−01	(10, 20)	1.325825214724776e+00
(11, 20)	8.769781368231594e−02	(12, 20)	−3.682847818679935e−03	(13, 20)	−3.922232926894130e−01
(14, 20)	7.273624441892870e−02	(23, 20)	2.500000000000000e−01	(24, 20)	2.500000000000000e−01
(25, 20)	−2.500000000000000e−01	(26, 20)	2.500000000000000e−01	(9, 21)	3.535533905932737e−01
(10, 21)	2.187611604295881e+00	(11, 21)	−5.593325124620151e−01	(12, 21)	2.347815484408458e−02
(13, 21)	2.502495092793016e+00	(14, 21)	−4.640388251536717e−01	(25, 21)	1.000000000000000e+00
(9, 22)	−1.325825214724776e−01	(10, 22)	−8.175922157469455e−01	(11, 22)	−2.085412577327513e−01
(12, 22)	8.746763569364843e−03	(13, 22)	9.336019220353635e−01	(14, 22)	−1.730938474779569e−01
(26, 22)	1.000000000000000e+00	(9, 23)	−7.733980419227862e−02	(10, 23)	−4.806116403377315e−01
(11, 23)	1.027514541411702e+00	(12, 23)	−1.712524235686170e−01	(13, 23)	−4.176349426383046e+00
(14, 23)	8.838834764831843e−01	(25, 23)	−5.000000000000013e−01	(26, 23)	−7.499999999999983e−01
(27, 23)	−7.407407407407403e−01	(28, 23)	4.444444444444446e−01	(29, 23)	8.888888888888903e−01
(30, 23)	−4.074074074074087e−01	(9, 24)	5.524271728019902e−02	(10, 24)	3.425048471372339e−01
(11, 24)	6.214805694022389e−01	(12, 24)	−1.114061465150680e−01	(13, 24)	−2.994155276586787e+00
(14, 24)	6.113527379008691e−01	(25, 24)	2.499999999999989e−01	(26, 24)	2.500000000000019e−01
(27, 24)	−4.444444444444445e−01	(29, 24)	1.000000000000002e+00	(30, 24)	−4.444444444444462e−01
(11, 25)	1.089662598351926e+00	(12, 25)	4.681820289496868e−01	(13, 25)	−8.452135743870448e−01
(14, 25)	−8.838834764831893e−02	(27, 25)	1.000000000000000e+00	(11, 26)	−6.062888221501843e−01
(12, 26)	2.260347848714810e−01	(13, 26)	3.541058177660758e+00	(14, 26)	−7.770808897414662e−01
(28, 26)	1.000000000000000e+00	(11, 27)	−5.569846969776066e+00	(12, 27)	4.539570292500355e+00
(13, 27)	4.224410590416819e+01	(14, 27)	−8.960368742848281e+00	(27, 27)	−2.222222222222204e−01
(28, 27)	−3.333333333333355e−01	(29, 27)	−2.666666666666670e+00	(30, 27)	1.777777777777781e+00
(11, 28)	6.053220745977807e+00	(12, 28)	−4.788162520261248e+00	(13, 28)	−5.086196979987922e+01
(14, 28)	1.186613567178675e+01	(27, 28)	−2.592592592592600e−01	(28, 28)	−4.444444444444452e−01
(29, 28)	−8.888888888888912e−01	(30, 28)	−5.925925925925908e−01	(11, 29)	−3.082543624235105e+00
(12, 29)	2.390858768289280e+00	(13, 29)	2.256941214482530e+01	(14, 29)	−4.735221582867724e+00
(29, 29)	1.000000000000000e+00	(11, 30)	−7.734325686210864e+00	(12, 30)	5.887147327154208e+00
(13, 30)	5.393208381272626e+01	(14, 30)	−1.088557744006321e+01	(30, 30)	1.000000000000000e+00

References

[AHJP] L. Andersson, N. Hall, B. Jawerth, G. Peters (1994): *Wavelets on closed subsets of the real line*. In: Topics in the Theory and Applications of Wavelets (L. L. Schumaker, G. Webb, eds.). Boston: Academic Press, pp. 1–61.

[CDP] J. M. Carnicer, W. Dahmen, J. M. Peña (1996): *Local decomposition of refinable spaces*. Appl. Comput. Harmonic Anal., **3**:127–153.

[CQ] C. K. Chui, E. Quak (1992): *Wavelets on a bounded interval*. In: Numerical Methods of Approximation Theory (D. Braess, L. L. Schumaker, eds.). Boston: Birkhäuser, pp. 1–24.

[CDF] A. Cohen, I. Daubechies, J.-C. Feauveau (1992): *Biorthogonal bases of compactly supported wavelets*. Comm. Pure Appl. Math., **45**:485–560.

[CDV] A. Cohen, I. Daubechies, P. Vial (1993): *Wavelets on the interval and fast wavelet transforms*. Appl. Comput. Harmonic Anal., **1**:54–81.

[D1] W. Dahmen (1994): *Some remarks on multiscale transformations, stability and biorthogonality*. In: Wavelets, Images and Surface Fitting (P. J. Laurent, A. Le Méhauté, L. L. Schumaker, eds.). Wellesley: A. K. Peters, pp. 157–188.

[D2] W. Dahmen (1996): *Stability of multiscale transformations*. J. Fourier Anal. Appl., **4**:341–362.

[D3] W. Dahmen (1995): *Multiscale analysis, approximation, and interpolation spaces*. In: Approximation Theory VIII (C. K. Chui, L. L. Schumaker, eds.). Singapore: World Scientific, pp. 47–88.

[D4] W. Dahmen (1997): *Wavelet and multiscale methods for operator equations*. Acta Numer., **6**: 55–228.

[DKU1] W. Dahmen, A. Kunoth, K. Urban (1999): *Biorthogonal spline-wavelets on the interval—Stability and moment conditions*. Appl. Comput. Harmonic Anal., **6**:132–196.

[DKU2] W. Dahmen, A. Kunoth, K. Urban (1997): *Wavelets in numerical analysis and their quantitative properties*. In: Surface Fitting and Multiresolution Methods (A. Le Méhauté, C. Rabut, L. L. Schumaker, eds.). Nashville, TN: Vanderbilt University Press, pp. 93–130.

[DM] W. Dahmen, C. A. Micchelli (1997): *Biorthogonal wavelet expansions*. Constr. Approx., **13**:293–328.

[DS] W. DAHMEN, R. SCHNEIDER (to appear): *Composite wavelet bases for operator equations*. Revised version, Preprint TU Chemnitz, December 1997. Math. Comp.

[GHM] J. S. GERONIMO, D. P. HARDIN, P. R. MASSOPUST (1994): *Fractal functions and wavelet expansions based on several scaling functions*. J. Approx. Theory, **78**:373–401.

[GY] S. S. GOH, V. B. YAP (1998): *Matrix extension and biorthogonal wavelet construction*. Linear Algebra Appl., **269**:139–157.

[GL] T. N. T. GOODMAN, S. L. LEE (1994): *Wavelets of multiplicity r*. Trans. Amer. Math. Soc., **342**: 307–324.

[HSS] C. HEIL, G. STRANG, V. STRELA (1996): *Approximation by translates of refinable functions*. Numer. Math., **73**:75–94.

[J] R. Q. JIA (1998): *Convergence of vector subdivision schemes and construction of biorthogonal multiple wavelets*. In: Advances in Wavelets (K. S. Lau, ed.). New York: Springer-Verlag, pp. 189–216.

[JM] R. Q. JIA, C. A. MICCHELLI (1992): *On linear independence of integer translates of a finite number of functions*. Proc. Edinburgh Math. Soc., **36**:69–85.

[JRZ1] R. Q. JIA, S. RIEMENSCHNEIDER, D. X. ZHOU (1997): *Approximation by multiple refinable functions*. Canad. J. Math., **49**:944–962.

[JRZ2] R. Q. JIA, S. RIEMENSCHNEIDER, D. X. ZHOU (1998): *Vector subdivision schemes and multiple wavelets*. Math. Comp., **67**:1533–1563.

[JRZ3] R. Q. JIA, S. RIEMENSCHNEIDER, D. X. ZHOU (to appear): *Smoothness of multiple refinable functions and multiple wavelets*. SIAM J. Matrix Anal. Appl.

[JS] R. Q. JIA, Z. W. SHEN (1994): *Multiresolution and wavelets*. Proc. Edinburgh Math. Soc., **37**: 271–300.

[P] G. PLONKA (1997): *Approximation order provided by refinable function vectors*. Constr. Approx., **13**:221–244.

[PS1] G. PLONKA, V. STRELA (1998): *Construction of multiscaling functions with approximation and symmetry*. SIAM J. Math. Anal., **29**:481–510.

[PS2] G. PLONKA, V. STRELA (1998): *From wavelets to multiwavelets*. In: Mathematical Methods for Curves and Surfaces II (M. Dæhlen, T. Lyche, L. Schumaker, eds.). Nashville, TN: Vanderbilt University Press.

[SS1] G. STRANG, V. STRELA (1995): *Short wavelets and matrix dilation equations*. IEEE Trans. Signal Process, **43**: 108–115.

[SS2] G. STRANG, V. STRELA (1997): *Pseudo-biorthogonal multiwavelets and finite elements*. Manuscript.

[Y] H. YSERENTANT (1986): *On the multilevel splitting of finite element spaces*. Numer. Math., **49**: 379–412.

W. Dahmen, A. Kunoth
Institut für Geometrie und Praktische Mathematik
RWTH Aachen
52056 Aachen
Germany
{dahmen,kunoth}@igpm.rwth-aachen.de,
WWW: http://www.igpm.rwth-aachen.de/
~{dahmen,kunoth}

R.-Q. Jia
Department of Mathematical Sciences
University of Alberta
Edmonton
Canada T6G 2G1
{bhan,jia}@math.ualberta.ca,
WWW: http://www.math.ualberta.ca/
~{bhan,jia}

B. Han
Program in Applied and Computational Mathematics
Princeton University
Princeton, NJ 08544
USA
bhan@princeton.edu
bhan@xihu.math.ualberta.ca